

國立交通大學
電機與控制工程學系

碩士論文

即時車輛導航系統之 GPS/INS/GIS 整合設計



Design of GPS/INS/GIS for a
Real-Time Vehicle Navigation System

研究生：楊世宏

指導教授：陳永平 教授

中華民國九十三年六月

即時車輛導航系統之 GPS/INS/GIS 整合設計

Design of GPS/INS/GIS for a Real-Time Vehicle Navigation System

研 究 生：楊世宏

Student : Shih-Hung Yang

指 導 教 授：陳永平 教授

Advisor : Professor Yon-Ping Chen



A Thesis

Submitted to Department of Electrical and Control Engineering

College of Electrical Engineering and Computer Science

National Chiao Tung University

In Partial Fulfillment of the Requirements

For the degree of Master

In

Electrical and Control Engineering

June 2004

Hsinchu, Taiwan, Republic of China

中華民國九十三年六月

即時車輛導航系統之 GPS/INS/GIS 整合設計

學生：楊世宏

指導教授：陳永平 教授

國立交通大學電機與控制工程學系



本論文提出一套以卡爾曼濾波器整合全球定位系統與慣性導航系統的即時車輛導航系統，再利用地圖匹配演算法消除來自卡爾曼濾波器的誤差，且找到正確的道路與位置。此硬體架構整合一個加速規與一個陀螺儀量測二維位移、速度、車頭方向，同時設計了兩個微算器以擷取全球定位系統接收器與慣性量測元件之資料，然後傳送到主處理器運算。接著主處理器利用卡爾曼濾波器來估算最佳導航資訊。此外本論文提出一個修正的地圖匹配演算法以調整車頭方向。最後最佳導航資訊將會顯示在使用者之圖示介面。實驗結果將證實提出的方法對於車輛行經都市區、地下道、樹林茂盛的地區時是有效且可實現的。

Design of Integrated GPS/GIS for a Real-Time Vehicle Navigation System

Student: Shih-Hung Yang

Advisor: Professor Yon-Ping Chen

Department of Electrical and Control Engineering

National Chiao Tung University

The logo of National Chiao Tung University is a circular emblem with a gear-like outer border. Inside the circle, there is a stylized building and the year '1896' at the bottom. The word 'ABSTRACT' is overlaid in the center of the logo.

ABSTRACT

In this thesis, a GPS/INS navigation system integrated by Kalman Filter is proposed. Furthermore, a map-matching algorithm that eliminates the error of GPS/INS and finds the correct road and position on the map is also applied to this real-time vehicle navigation system. One accelerometer and one gyro are integrated in the system to obtain 2-D displacement, velocity, and heading direction. Two microprocessors are designed to capture both the signals of GPS receiver and IMU set, and then transmit data to the main processor. After that, the optimal navigation information of GPS/INS is estimated in the main processor by the Kalman filter. In addition, a modified map-matching algorithm is adopted to adjust the heading direction of vehicle. Finally, the optimal navigation information would be shown in a graphical user interface. The experiment results would demonstrate the effectiveness and applicability of the proposed methods as the vehicle runs in the urban area, underground passage, and wooded area.

Acknowledgment

在兩年的研究過程中，首先要感謝我的指導老師陳永平教授，教導我們正確的研究方法、態度以及解決問題的能力，在研究同時，也親自批改我們的論文，增長我們英文寫作能力，此外，也感謝忠隆、佳宏學長，儘管畢業在外工作，也不時幫助我的研究，在實驗上，更要感謝翰宏同學開車進行實驗，成果才會如此完美。

研究所兩年中，很感謝室友智傑的鼓勵，不管在學業、研究、生活，都能彼此互相鼓勵、扶持，也謝謝實驗室的伙伴，尤其是一起畢業的翰宏、依娜、智淵、倉鴻、培瑄，生活中有了你們的陪伴，才能如此快樂，還有手語 91 的同伴們，彼此關懷近況，也謝謝 Campus 的鼓舞以及生活上的支持，這本論文富含著你們的色彩，最後，我要感謝我的家人，給予無時無刻的照顧。

僅以此篇獻給所有關心、照顧我的朋友們。



楊世宏 2004/7/6

Contents

Chinese Abstract	i
English Abstract	ii
Acknowledgement	iii
Contents	iv
Index of Figures	vi
Index of Tables	viii
Chapter 1 Introduction	1
Chapter 2 Global Positioning System	3
2.1 Introduction	3
2.2 GPS Satellite Signals	4
2.3 GPS Navigation Message	6
2.4 GPS Observations	7
2.4.1 Pseudo Range	7
2.4.2 Carrier Phase	8
2.5 GPS Error Sources	8
2.6 Position Accuracy and DOP	9
2.7 Differential GPS Technique	10
2.8 The Positioning Equation	11
Chapter 3 Inertial Navigation System	13
3.1 System Overview	13
3.1.1 Gimballed System	13
3.1.2 Strapdown System	14
3.2 Coordinate Frames and Transformation	15
3.2.1 Coordinate Frames	15
3.2.2 Transformation Between ECEF and Geodetic Frames	17
3.2.3 Transformation Between Body And Navigation Frames	19
3.3 Dynamic Equations In Navigation	21
3.3.1 Coordinate Transformation Matrix Properties	21



3.3.2 Velocity Dynamic Equation	23
3.4 INS Error Model	27
3.4.1 Error Model	27
3.4.2 Error Sources	29
3.4.3 The Reduced Error Model	33
Chapter 4 Geographic Information System	34
4.1 Introduction	34
4.2 Reference Ellipsoids and Projection	34
4.3 Taiwan Coordinates	37
4.4 Map-Matching Algorithm	38
4.4.1 Map Matching Issues	38
4.4.2 Map Matching Structure	40
4.4.3 Initial Mode	41
4.4.4 Node Nearby Detection and Searching Mode	41
4.4.5 Tracking Mode	44
Chapter 5 Integration of GPS/INS/GIS	45
5.1 Motivation	45
5.2 Integration Mode	46
5.3 Filter Design	50
5.3.1 Discrete Linear Dynamics Model and Observation Model	50
5.3.2 Optimal State Vector Estimation	52
5.4 Navigation System Design	54
5.4.1 Hardware and Software	54
5.4.2 Programming Procedure	56
5.5 Experiments	61
Chapter 6 Conclusions	67
References	70



List of Figures

Figure 2.1 Global Positioning System Overview	3
Figure 2.2 GPS Satellite Signals	5
Figure 2.3 GPS Navigation Data Format	6
Figure 2.4 Dilution of Precision	10
Figure 2.5 Differential GPS Technique	11
Figure 2.6 GPS Positioning Method	12
Figure 3.1 The gimballed INS system	14
Figure 3.2 Body (Vehicle) coordinate frame	15
Figure 3.3 Navigation frame or tangent plane reference coordinate frame	16
Figure 3.4 ECEF rectangular coordinate system	16
Figure 3.5 Geodetic reference coordinate system	17
Figure 3.6 Relation between body and navigation frame	19
Figure 3.7 Rotation by the Euler angles	20
Figure 3.8 Gravitational acceleration vector in the navigation frame	25
Figure 4.1 Semi-major axis and semi-minor axis	35
Figure 4.2 Projections and the appearance of the Graticules	36
Figure 4.3 Azimuthal projection	36
Figure 4.4 Projected errors	39
Figure 4.5 Dot-product	39
Figure 4.6 Moving distance	39
Figure 4.7 Map matching flowchart	40
Figure 4.8 Initial mode	41
Figure 4.9 Searching mode flowchart	42
Figure 4.10 Condition 2	43

Figure 4.11 Tracking mode	44
Figure 5.1 GPS/INS integration scheme	46
Figure 5.2 GPS/INS without GIS fix	47
Figure 5.3 GIS fix GPS/INS	48
Figure 5.4 Turn Detect Range	48
Figure 5.5 GIS fix GPS/INS	49
Figure 5.6 GPS/INS/GIS integration mode	49
Figure 5.7 Raw Map Data Format	55
Figure 5.8 Shapefile in ArcView	56
Figure 5.9 The data flowchart in two microprocessors	57
Figure 5.10 Heading direction estimation	59
Figure 5.11 Initialize heading direction for INS	59
Figure 5.12 Check position reliability	60
Figure 5.13 Path 1	62
Figure 5.14 Path 2	62
Figure 5.15 Path 1 result without GIS correction	63
Figure 5.16 Path 1 result with GIS correction	65
Figure 5.17 Path 2 result	66
Figure 5.18 Experiment equipment	66



List of Tables

Table 2.1 User equivalent range error (UERE)	11
Table 4.1 Ellipsoidal Parameters	35
Table 4.2 Selected reference ellipsoids	35
Table 4.3 Taiwan coordinates	37



Chapter 1 Introduction

In recent years, many research are devoted to the real-time car navigation systems. Some of them are concentrated on position estimation; some developed systems gave the shortest route. They are all expected to communicate with traffic management in the future.

The car navigation system mainly provides the position estimation. Dead reckoning and Inertial Navigation System (INS) has been adopted to estimate vehicle's position. They estimate position from integrating the displacement, acceleration, and angular rate at every sampling time. However, this estimated method would produce large error due to the fact that the error would be accumulated from surface roughness or sensor error for a long time. To remedy this problem, the Global Positioning System (GPS) attractive in car navigation system is employed to provide the absolute position every second if more than four satellites were observed.

However, the GPS is subject to the signal outage, interference, and jamming. On the contrary, INS is a self-contained and much immune to surrounding environment. The best way to obtain the optimal position estimation is to combine GPS and INS. In order to combine them, most researchers relied on Kalman filter, which is a recursive algorithm and requires external measurements to compute optimal corrections of system state variables. The assumptions in the use of Kalman filter are the system is linear and the noise is white Gaussian. However, the system model in INS is nonlinear and the noises of GPS and INS aren't Gaussian. The position estimation from Kalman filter is not optimal.

The map-matching algorithm is a useful method to eliminate the error according to the exact position in map, as reliable road maps are available. The map-matching algorithm is a scheme to find the road and position where the vehicle runs. The fact is

that the vehicle always runs on the road and the error from filter would be eliminate if the position of vehicle is known in the road on map. [11] However, this algorithm would leads to mapping error as the GPS signal is unavailable and the error accumulation from INS is too large.

In this thesis, a modified map-matching algorithm is proposed to solve this problem. This modified algorithm, heading direction estimation, employs the direction of road to adjust the heading direction of vehicle. Furthermore, as the vehicle makes a turn, the INS would measure the variation of angular rate and the GIS would detect if there were a node near the vehicle. There are some roads that are new built and don't updated in the GIS database. The proposed method would detect whether there were a road near the vehicle or not. If not, that means the GIS is fail, the GPS/INS trajectory would replace the matching point from GIS. The practical experiment would show the effectiveness and applicability of the proposed algorithm.

In chapter 2, the Global Positioning System (GPS) is presented to introduce how the GPS determine the absolute position. The chapter 3 will discuss the Inertial Navigation System (INS) and present the dynamic equation and error model in INS. In chapter 4, the geographic information system (GIS) is introduced to know the Taiwan coordinates and the map-matching algorithm. The chapter 5 will present the integration of GPS/INS/GIS and the proposed method, heading direction estimation, is provided. The real road experiment results are also shown in this chapter. Concluding remarks are given in chapter 6.

Chapter 2 Global Positioning System

2.1 Introduction

NAVSTAR GPS, an acronym standing for Navigation System with Timing and Ranging Global Positioning System, is designed to provide highly accurate, 24-hour and worldwide coverage for position reporting and created by the United States Department of Defense. The NAVSTAR GPS consists of three major segments:

- A. The space segment
- B. The user segment
- C. The control segment

Figure 2.1 shows the relations of three major segments.

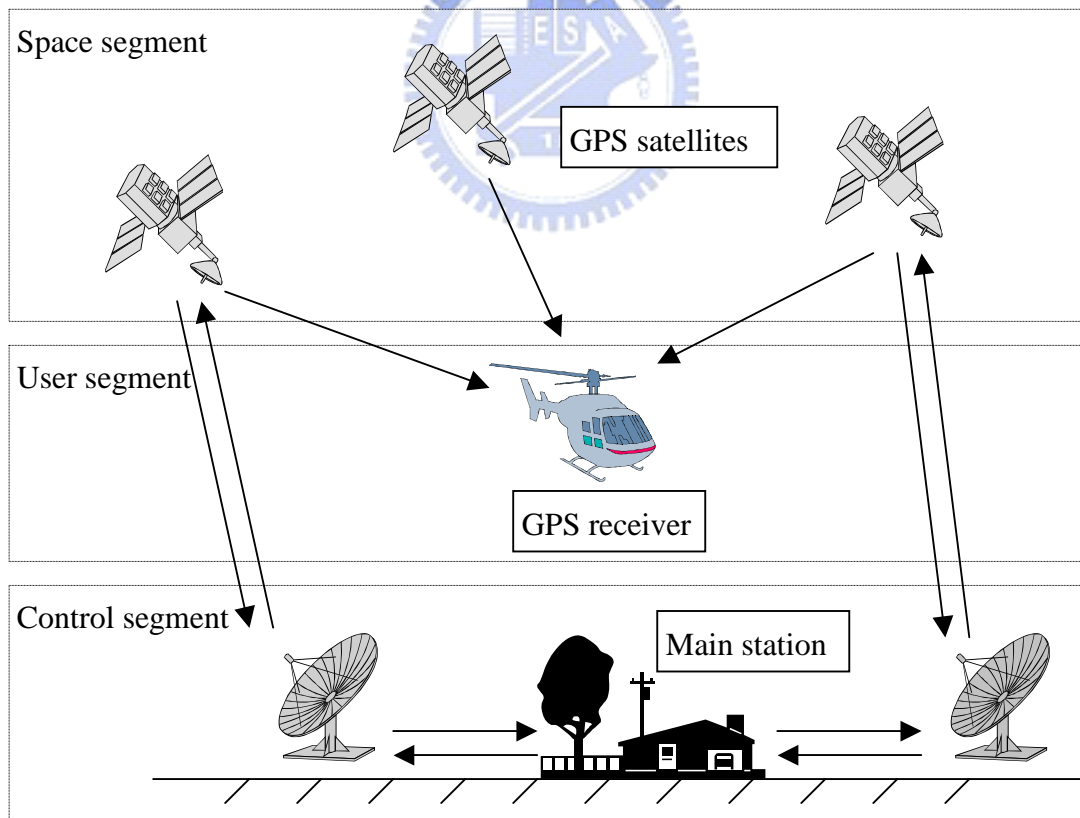


Figure 2.1 Global Positioning System Overview [23]

The space segment of the GPS includes 21 working satellites and 3 spares, and they are arranged in six nearly circular orbit planes, which contain four satellites each plane. The 24 spacecraft are placed in 20,200 km circular orbits inclined at 55 degrees and surround Earth with approximately 12 sidereal hours.

The control segment is made up of a master control station, worldwide monitor stations and ground control stations. These monitor stations track the satellites continuously all day, and they measure signals from the space vehicles (SVs), which are incorporated into orbital models for each satellite. The models compute precise orbital data (ephemeris) and SV clock data to the SVs. Then the SVs send subsets of the orbital ephemeris data to GPS receivers. Thus, the purpose of the control segment is to track the GPS satellites and correct ephemeris constants and clock-bias errors.

The user segment consists of the GPS receivers and the user community. As GPS receivers receive four satellites signals, the four dimensions, x , y , z , and time would be calculated from triangulation. The receiver measures the pseudo range and carrier phase from the satellite. Furthermore, the satellites provide two different accurate signals. Coarse-Acquisition Code (C/A) is used for civilian and Precision Code (P) provides more accurate positional precision.

2.2 GPS Satellite Signals

Each satellite transmits a unique coded signal that consists of the identification of the satellite and the ranges to it. The satellite signals based on two L-band frequencies centered on 1575.42 MHz (L1 frequency) and 1227.60 MHz (L2 frequency), which are derived from a fundamental clock frequency of 10.23 MHz. The L1 frequency carries the navigation message and the Standard Positioning Service (SPS) code signals. The L2 frequency is used to measure the ionospheric delay by Precise

Positioning Service (PPS) equipped receivers.

The C/A Code, which modulates the L1 carrier phase, is a repeating 1 MHz Pseudo Random Noise (PRN) code. This noise-like code modulates the L1 carrier signal to spreading the spectrum over 1 MHz bandwidth. Each SV has different C/A code PRN, i.e. satellites are identified with their PRN number.

The P-Code, is a 10 MHz PRN code, modulates both the L1 and L2 carrier phases. In the Anti-Spoofing (AS) mode of operation, the P-Code is encrypted into the Y-Code that is used by authorized users with cryptographic keys. Therefore, the C/A Code and P (Y)-Code are the basis of civil SPS and PPS respectively. Figure 2.2 schemes the structure of GPS satellite signals.

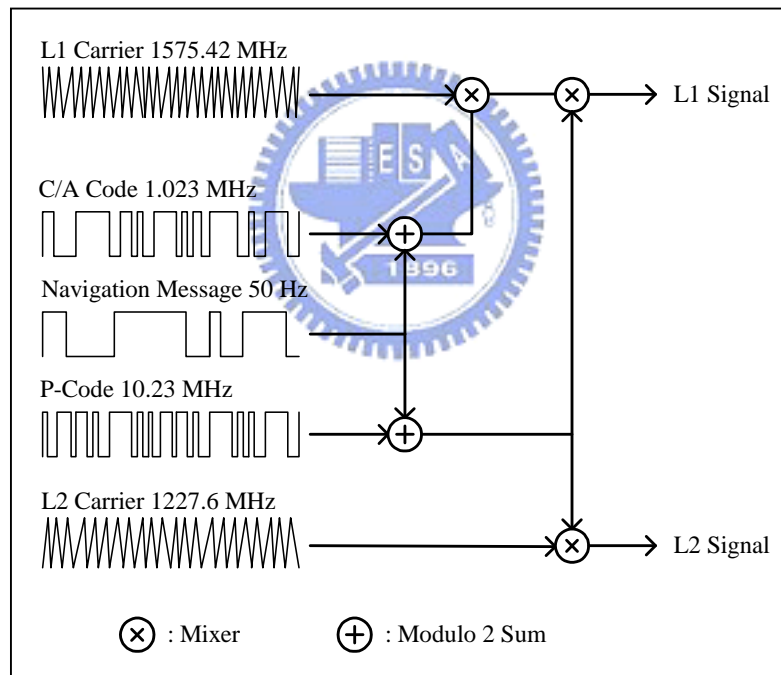


Figure 2.2 GPS Satellite Signals

2.3 GPS Navigation Message

GPS navigation message, a 50 Hz signal, consists of data bits that describe the GPS satellite orbits, clock corrections, and other system parameters. A data bit frame, which is transmitted every 30 seconds, consists of 1500 bits divided into five 300-bit subframes. The subframes 1, 2, and 3 contain orbital and clock data where subframe 1 send SV clock corrections and subframes 2 and 3 send precise SV orbital data sets (ephemeris data parameters). Furthermore, subframes 4 and 5 transmit different pages of system data. In addition, each subframe comprises the telemetry word (TLW) and the handover word (HOW). TLW tells the receiver what the subframe data received, and HOW provides the information of TOW (Time Of Week) that helps the locked P code word. Figure 2.3 shows the scheme of relations between each data format in GPS navigation message.

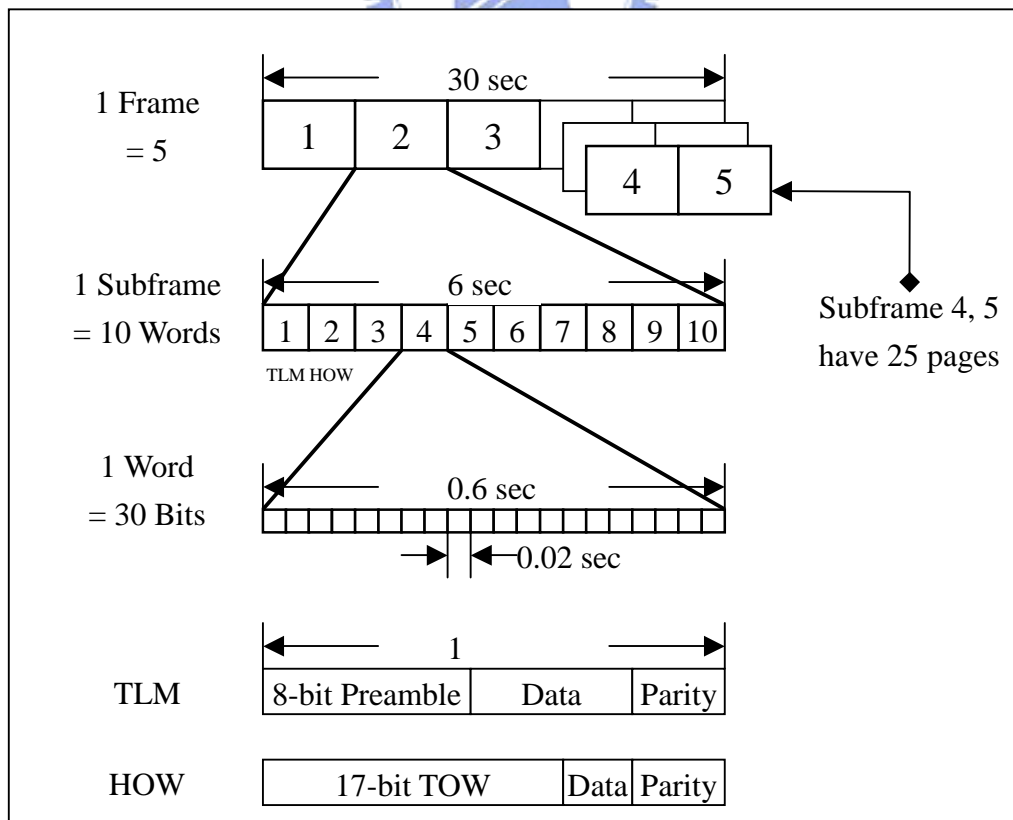


Figure 2.3 GPS Navigation Data Format

2.4 GPS Observations

There are two fundamental observations, pseudo range and carrier phase, which can determine the user location. In general, the pseudo range, the main positioning tool, is utilized with less computation, and the carrier phase is always used in high precision surveying that costs a lot of time to obtain the high precision position. The two observations would be presented in the following sections.

2.4.1 Pseudo Range

The pseudo range measures the distance by decoding the P or C/A code at the epochs between transmitting and receiving the signals. In fact, because the clock of the satellites and the receivers are asynchronous, this method is not achievable and timing errors might be cause. Not only the asynchronous effect, but the tropospheric and ionospheric propagation delays also affect the measurement of pseudo range. Thus, the general expression of pseudo range can be interpreted as: [23]

$$PR = R + c \cdot (\Delta t_r - \Delta t_s) + c \cdot \Delta t_a \quad (2.4.1)$$

where

PR : Pseudo range

R : True range

c : Light speed

Δt_r : Receiver clock bias

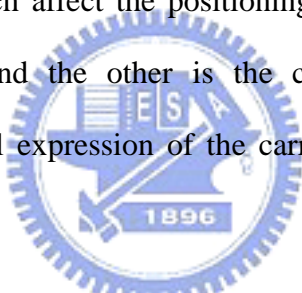
Δt_s : Satellite clock bias

Δt_a : Atmospheric propagation delay

2.4.2 Carrier Phase

Carrier phase tracking GPS signals requires specially equipped carrier tracking receivers and has a revolution in land surveying. L1 and L2 cycles have wavelengths of 19 and 24 centimeters respectively. These carrier signals can provide ranging measurements with around millimeters accuracy under special circumstances. However, it always costs much time to get high precision position, and therefore the carrier phase is generally used in surveying.

The carrier phase observation is still affected from the receiver clock error and the atmospheric propagation. Furthermore, as using carrier phase observation, there would be two problems, which affect the positioning accuracy. One is the cycle or phase ambiguity problem, and the other is the cycle slips problem. With the description above, the general expression of the carrier phase observation equation can be shown as: [23]


$$\varphi = \frac{f}{c} \cdot [R + c \cdot (\Delta t_r + \Delta t_a - \Delta t_s)] + N + \varepsilon_\varphi \quad (2.4.2)$$

where

φ : Carrier phase observation.

f : Carrier wave frequency.

N : Cycle ambiguity.

ε_φ : Other noise.

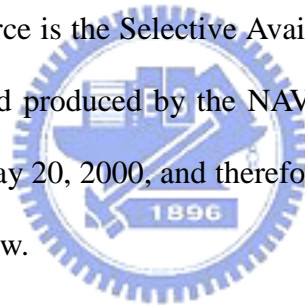
2.5 GPS Error Sources

The accuracy of GPS position measurements depends on the quality of the pseudo range measurements and satellite ephemeris data. The major error factors that

affect the accuracy of the GPS measurements are: [24]

- A. Satellite clock errors
- B. Ephemeris errors (satellite position errors)
- C. Receiver errors
- D. Ionosphere errors (upper atmosphere errors)
- E. Troposphere errors (lower atmosphere errors)
- F. Multipath errors (errors from bounced signals)
- G. Selective Availability errors

The main GPS error source is the Selective Availability errors that are the signal transmission perturbations and produced by the NAVSTAR managers. However, the SA errors were removed at May 20, 2000, and therefore the GPS positioning accuracy can be up to 10~20 m level now.



2.6 Position Accuracy and DOP [24]

Dilution of Precision (DOP) is a value, which is the exception quality of position measurement based solely on the geometric arrangement of the satellites and the receiver being used for the measurement. When DOP value is unity, the accuracy is as good as it can be considering all the sources of error. This might occur when one satellite is overhead and the three others located in the horizon with 120 degrees to each other. Figure 2.4 shows the scheme of DOP. The overall DOP number includes several sub-DOPs:

- A. HDOP (Horizontal DOP) is a combination of NDOP (North DOP) and EDOP (Earth DOP).

B. VDOP (Vertical DOP).

C. PDOP (Position DOP) is a combination of HDOP and VDOP.

D. TDOP (Time DOP).

E. GDOP (Geometric DOP) is a combination of PDOP and TDOP.

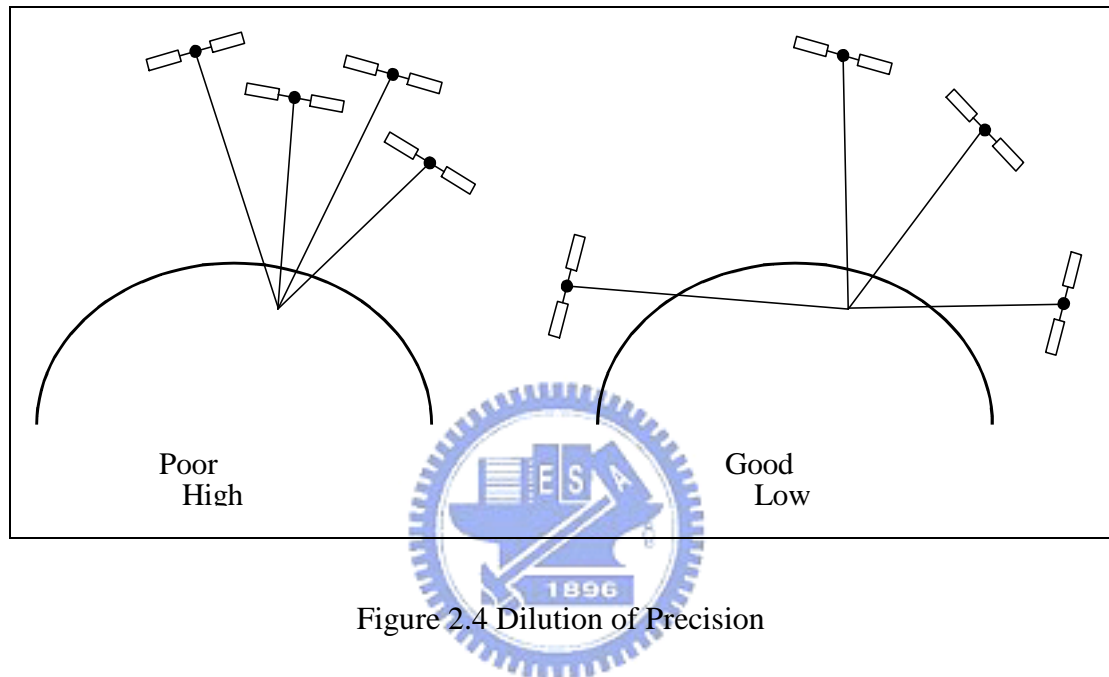


Figure 2.4 Dilution of Precision

2.7 Differential GPS Technique

All receivers in the same local geographic area have similar qualities of errors outlined in the section 2.5. Thus, the Differential GPS (DGPS) employs this characteristic and attempts to compensate the other receivers with a base station, whose accurate position is known, situated at a precisely surveyed location. This base station, like all other receivers, obtains signals and errors from the satellites and determines the range errors by differencing the calculated and the measured ranges. Then, these errors are broadcast to other receivers in the same local geographic area, so that the range measurements of receivers can be corrected and the more accurate position estimate can be also obtained. [23] Figure 2.5 shows that the reference station

receives and calculates the errors, and then transmits errors to the other receivers to correct the position error. Table 2.1 shows the set of error sources between GPS and DGPS. It is clear that DGPS is more accurate than GPS.

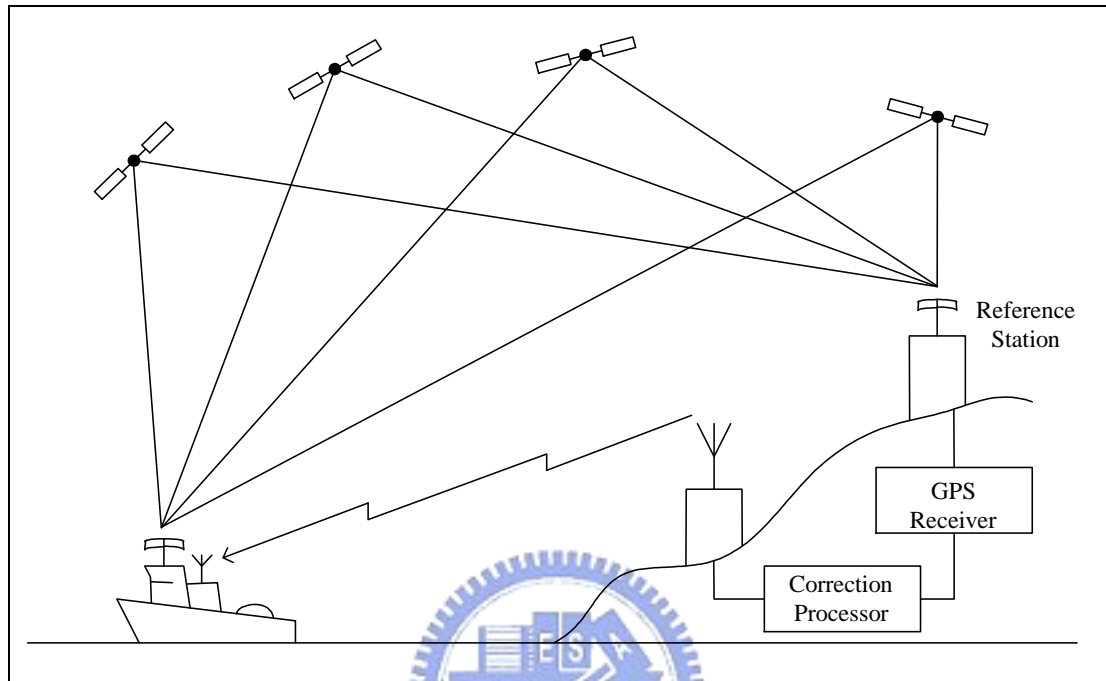


Figure 2.5 Differential GPS Technique

Table 2.1 User equivalent range error (UERE) [11]

Error Sources	Predicted Error (m)			
	GPS		DGPS	
	P code	C/A code	P code	C/A code
Satellite ephemeris error	2.62	2.62	0	0
Satellite clock error	3.48	3.48	0	0
Multipath error	1.22	3.48	1.22	3.48
Ionosphere error	0.4	6.4	0.15	0.15
Troposphere error	0.4	0.4	0.15	0.6
Receiver error	0.24	2.45	0.24	2.45
User ranging error (RMS)	4.25	8.54	1.28	3.96

2.8 The Positioning Equation

This section would present how to determine the coordinate and time from observing four satellites. When the satellites are observed, each satellite signal can provide its position (x_i, y_i, z_i) and the PRN code time T_i shown as figure 2.6. The

position (x, y, z) and the clock bias ΔT_{UCB} of the receiver can be solved by using the signal provided from each observed satellite. Thus, the basic observable equation can be shown as follows: [10]

$$R_i = c \times (\Delta T_i - \Delta T_{UCB}) = \sqrt{(x_i - x)^2 + (y_i - y)^2 + (z_i - z)^2} \quad i = 1, 2, 3, 4 \quad (2.8.1)$$

where

R_i : Pseudo range between receiver and the i^{th} observable satellite.

c : Light speed.

ΔT_i : PRN code delay time.

(x_i, y_i, z_i) : Position of the i^{th} observable satellite.

From the equation above, the position (x, y, z) and the clock bias ΔT_{UCB} of the receiver can be solved.

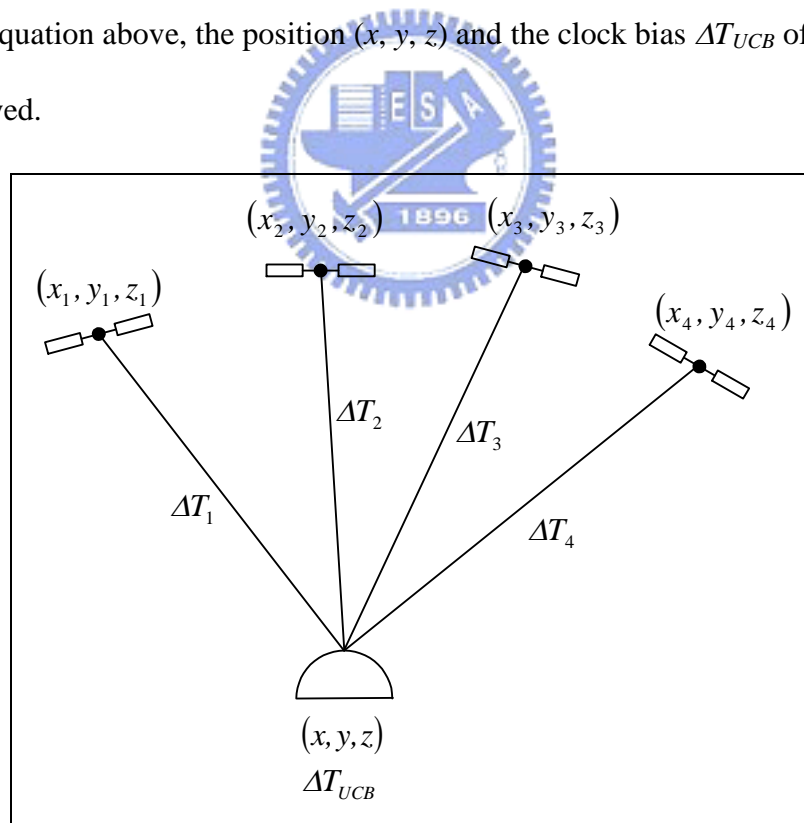


Figure 2.6 GPS Positioning Method

Chapter 3 Inertial Navigation System

Inertial Navigation System (INS) has been developed for a wide range of vehicles. In general, an INS is mainly built up by a set of inertial measurement units (IMU), which consists of accelerometers and gyros, and the IMU is mounted on a platform. Besides, a processor is required to transform the measured data of acceleration and angular rate into useful navigation information: position, velocity, and attitude. [3] However, INS inevitably has its disadvantage in the errors of position, velocity, and attitude, which are usually caused by alignment, measurement, calculation, and initial states and often accumulate and grow divergently with time in the integral process. Therefore, INS needs external sensor to compensate, and the most popular method is using GPS to correct the divergent error in INS.

INS can provide continuously position interpolation during the period of receiving GPS signal. The other purpose of INS would be used in automatic car control and that is to provide the velocity of vehicle, then the velocity would be feedback to control the vehicle.

3.1 System Overview

There are two general types of INS, gimballed and strapdown, which will be described in this section.

3.1.1 Gimballed System

Figure.3.1 shows the gimballed system, where the accelerometers and gyros are mounted on a stabilized platform system; hence, it is also called the stabilized platform system [18]. To be a stabilized reference coordinates, the gimbals should be well controlled and then isolated from the vehicle's motion. Furthermore, the

accelerometers can be horizontally aligned to get rid of the gravity effect by rotating the platform. Although the gimballed system has high accuracy, some disadvantages, such as complex hardware design, high cost, and large power consuming, make the design of this system difficult.

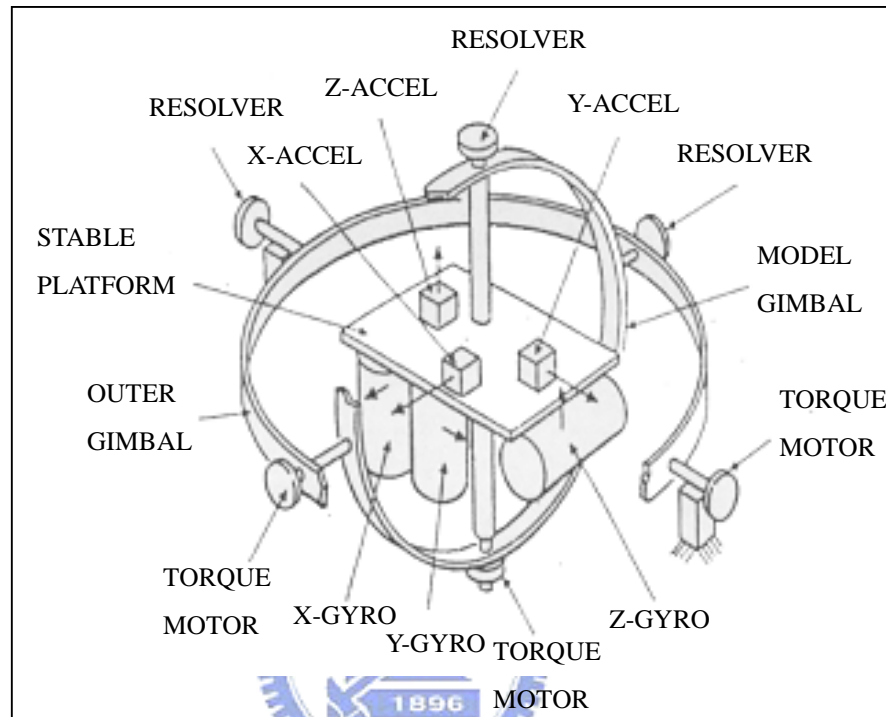


Figure 3.1 The gimballed INS system

3.1.2 Strapdown System

Contrary to gimballed INS system, the accelerometers and gyros (IMU) are mounted on a platform fixed on the vehicle in strapdown INS (SDINS). The IMU can measure the acceleration and angular velocity of vehicle, which are used to calculate the variation of position, velocity, and attitude. In the computing process, numerical errors caused by integrating the accelerations and angular rates would be produced accumulatively and divergently. Besides, the calculation of DCM (Direct cosine matrix) and Euler angle is quite complicated such that a high-performance processor is often needed. Fortunately, the technology of processor has been increasingly improved and good enough to do this work.

It is known that the gimballed INS system, better than the SDINS in accuracy, is commonly adopted for long-term navigation. However, the SDINS is generally employed for short-term navigation due to its small size, low cost, power saving, and easy design. For car-navigation, Hence the SDINS is available for car-navigation, which requires short-term data, with external sensors, like GPS, which can compensate the disadvantages in long-term work.

3.2 Coordinate Frames And Transformation

In general, there are five coordinate frames commonly used in an inertial navigation system. This section will first briefly describe these five coordinate systems and then show two transformations, between body and navigation frames and between geodetic and Earth-centered earth-fixed frames.

3.2.1 Coordinate Frames



A. Body Frame

The body frame, also called the vehicle coordinate frame, is symbolized as b -frame. The measurements acquired by various inertial sensors can easily apply to the body frame. Usually, the body frame is rigidly attached to the vehicle's center of gravity and its three axes are conventionally defined along the forward, right, and down directions as shown in Figure. 3.2, especially when adopted for car navigation.

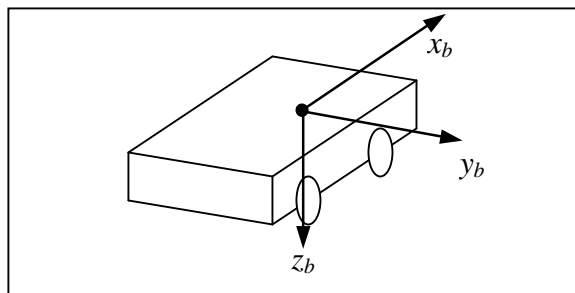


Figure 3.2 Body (Vehicle) coordinate frame

B. Navigation Frame [3]

The navigation frame, denoted as n -frame, is also called local geodetic frame with origin fixed on the vehicle and three axes pointing to the true north, east, and down as shown in Figure. 3.3. Clearly, the navigation frame intrinsically moves with the vehicle and then it is not suitable for specifying the vehicle's position on the earth. In fact, this frame plays a main role to provide local north, east, down directions and velocities, which is useful for navigation systems with sensors generally aligned with the local horizontal and vertical planes.

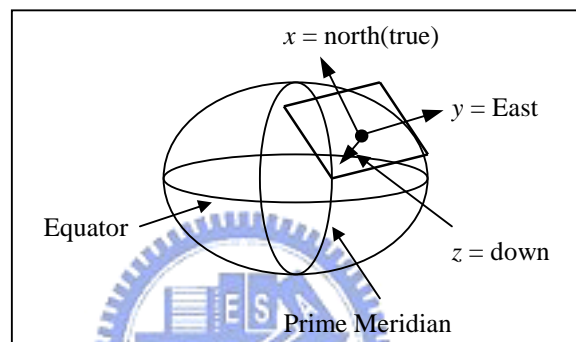


Figure 3.3 Navigation frame or tangent plane reference coordinate frame

C. Earth-Centered Earth-Fixed (ECEF) Frame

The earth-centered earth-fixed frame, which is symbolized as e -frame, is constructed with origin at the earth's mass center and the three axes rotate with earth. Furthermore, WGS-84 (World Geodetic System, 1984) is one kind of ECEF frame. Besides, the x -axis and the y -axis respectively point to the prime meridian of 0° longitude and the meridian of 90° longitude through the tangent plane of the equator, and the z -axis points to North Pole as shown in Figure. 3.4.

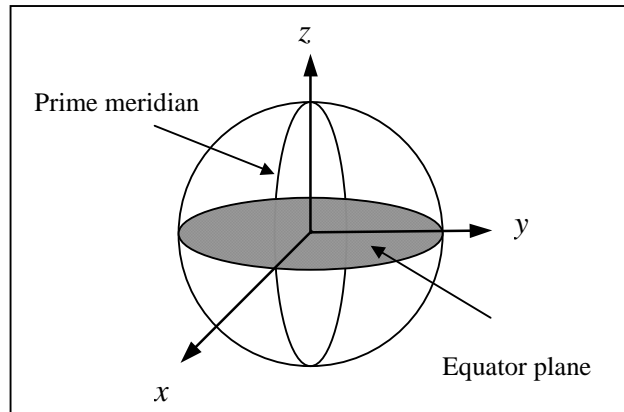


Figure 3.4 ECEF rectangular coordinate system

D. Geodetic Frame

The geodetic frame, which is symbolized as g -frame, describes the position of a moving body by the longitude, latitude, and altitude, denoted as l , L , and h , where the 0° longitude is defined at Greenwich meridian and the 0° latitude is defined at the equator. The meridian longitudes start from 0° longitude at Greenwich meridian to the west and the east each up to 180° and the parallel latitudes start from 0° latitude at the equator to the north and the south each up to 90° . The altitude is defined as a distance from the local sea level to the point where the vehicle locates as shown in Figure 3.5.

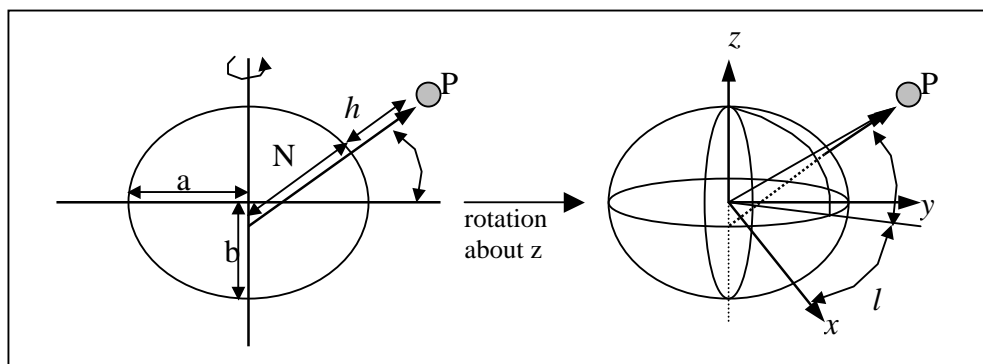


Figure 3.5 Geodetic reference coordinate system

E. Inertial frame

This frame is the most fundamental coordinate system that is symbolized as i -frame and defined in which Newton's laws of motion apply. The frame is static or in uniform linear motion system without accelerating. The definitions of axes are

generally built base on the star in universe. The x and z axes point toward the vernal equinox and along the earth's spin axis. The y -axis is defined to complete the right-handed coordinate system. In this analysis, the frame is attached to the center of earth, and is not rotating.

3.2.2 Transformation Between ECEF and Geodetic Frames

This section will discuss the transformation between ECEF and geodetic (Longitude, Latitude, and Altitude)[17]. Besides, the WGS-84 ellipsoid parameters are used throughout this discussion. The position in the ECEF frame is calculated as follows.

$$x = (N+h) \cdot \cos(L) \cdot \cos(l) \quad (3.2.1)$$

$$y = (N+h) \cdot \cos(L) \cdot \sin(l) \quad (3.2.2)$$

$$z = [N(1-e^2) + h] \cdot \sin(L) \quad (3.2.3)$$

where

$$N(L) = \frac{a}{\sqrt{1 - e^2 \sin^2(L)}} \quad (3.2.4)$$

Semimajor axis length: $a = 6378137.0\text{m}$

Semiminor axis length: $b = 6356752.3142\text{m}$

Eccentricity: $e = 0.0818$

In GPS application, the range measurements of GPS receiver are determined in ECEF frame. However, the information of geodetic frame is more useful in navigation. Therefore, the transformation between ECEF and geodetic frame is desired to solve. Longitude (l) can be solved as

$$l = \arctan 2(y, x) \quad (3.2.5)$$

The solutions of h and L can be computed by iterations as follows:

A. Initialization:

Let

$$h = 0$$

$$N = a$$

$$p = \sqrt{(x^2 + y^2)}$$

B. Perform the following iteration until convergence:

$$\sin(L) = \frac{z}{N(I - e^2) + h}$$

$$L = \arctan\left(\frac{z + e^2 N \sin(L)}{p}\right)$$

$$N = \frac{a}{\sqrt{1 - e^2 \sin^2(L)}}$$

$$h = \frac{p}{\cos(L)} - N$$



3.2.3 Transformation Between Body and Navigation Frames

In vehicle navigation application, the relation between body frame (x, y, z) and navigation frame (N, E, D) is shown in Figure 3.6. This relation exists angular motion between body and navigation frame. Therefore, the transformation between them will be discussed in this section.

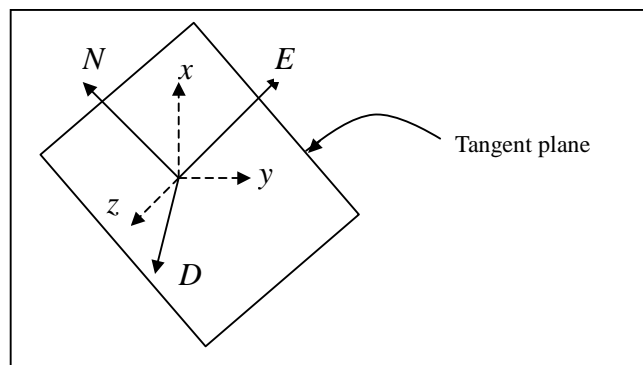


Figure 3.6 Relation between body and navigation frame

Consider the three rotations involving the Euler angles $(\phi, \theta, \psi) = (\text{roll}, \text{pitch}, \text{yaw})$.

A. Rotates the navigation frame by ψ radians about the D axis as shown in Figure 3.7 (a).

$$\begin{bmatrix} x' \\ y' \\ z' \end{bmatrix} = \begin{bmatrix} \cos\psi & \sin\psi & 0 \\ -\sin\psi & \cos\psi & 0 \\ 0 & 0 & 1 \end{bmatrix} \begin{bmatrix} N \\ E \\ D \end{bmatrix} \quad (3.2.6)$$

B. The second rotation rotates the coordinate that resulted from previous yaw rotation by θ radians about the y' axis as shown in Fig 3.7 (b).

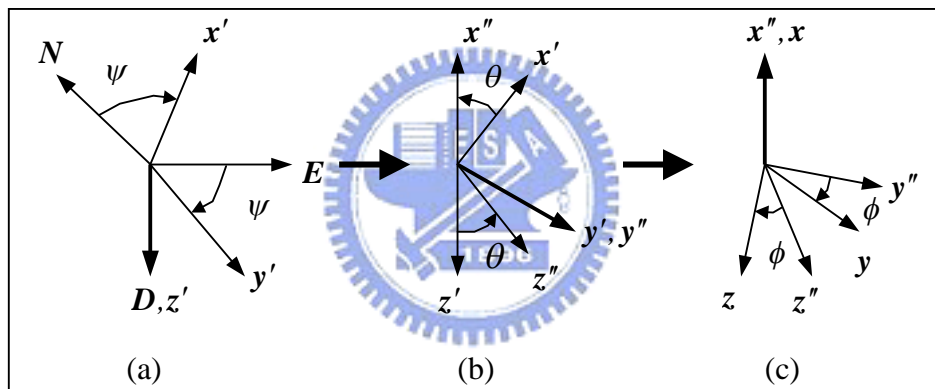


Figure 3.7 Rotation by the Euler angles

$$\begin{bmatrix} x'' \\ y'' \\ z'' \end{bmatrix} = \begin{bmatrix} \cos\theta & 0 & -\sin\theta \\ 0 & 1 & 0 \\ \sin\theta & 0 & \cos\theta \end{bmatrix} \begin{bmatrix} x' \\ y' \\ z' \end{bmatrix} \quad (3.2.7)$$

C. The third rotation rotates the coordinate that resulted from previous pitch rotation by ϕ radians about the x'' axis as shown in Fig 3.7 (c).

$$\begin{bmatrix} x \\ y \\ z \end{bmatrix} = \begin{bmatrix} 1 & 0 & 0 \\ 0 & \cos\phi & \sin\phi \\ 0 & -\sin\phi & \cos\phi \end{bmatrix} \begin{bmatrix} x'' \\ y'' \\ z'' \end{bmatrix} \quad (3.2.8)$$

The vector represented in tangent-plane coordinate can be transformed into body-frame by the transformation described as

$$\begin{bmatrix} x \\ y \\ z \end{bmatrix} = \mathbf{C}_t^b \begin{bmatrix} N \\ E \\ D \end{bmatrix} \quad (3.2.9)$$

where

$$\mathbf{C}_t^b = \begin{bmatrix} 1 & 0 & 0 \\ 0 & \cos \phi & \sin \phi \\ 0 & -\sin \phi & \cos \phi \end{bmatrix} \begin{bmatrix} \cos \theta & 0 & -\sin \theta \\ 0 & 1 & 0 \\ \sin \theta & 0 & \cos \theta \end{bmatrix} \begin{bmatrix} \cos \psi & \sin \psi & 0 \\ -\sin \psi & \cos \psi & 0 \\ 0 & 0 & 1 \end{bmatrix}$$

$$= \begin{bmatrix} \cos \psi \cos \theta & \sin \psi \cos \theta & -\sin \theta \\ -\sin \psi \cos \phi & \cos \psi \cos \phi & \cos \theta \sin \phi \\ +\cos \psi \sin \theta \sin \phi & +\sin \psi \sin \theta \sin \phi & \cos \theta \sin \phi \\ \sin \psi \sin \phi & -\cos \psi \sin \phi & \cos \theta \cos \phi \\ +\cos \psi \sin \theta \cos \phi & +\sin \psi \sin \theta \cos \phi & \cos \theta \cos \phi \end{bmatrix} \quad (3.2.10)$$

Furthermore, the transformation \mathbf{C}_b^t is determined as $(\mathbf{C}_t^b)^T$.

3.3 Dynamic Equations in Navigation

Generally, navigation problem is based on integrating sensed accelerations and angular rates to solve position, velocity, and attitude. In n -frame, there are a lot of differential nonlinear equations, based on the dynamics of motion according to Newton's Law, which can be formulated and constitute dynamic equations. In this section, the dynamic equations will be derived. In order to realize the dynamic equations, two fundamental concepts and properties should be discussed and expounded, and then dynamic equations can be derived easily.

3.3.1 Coordinate Transformation Matrix Properties

Consider the position of a point represented by a -frame and b -frame. The transformation of the a -frame to b -frame can be written as

$$\mathbf{r}^b = \mathbf{C}_a^b \mathbf{r}^a \quad (3.3.1)$$

where \mathbf{r}^a and \mathbf{r}^b are respectively the position vectors in a -frame and b -frame and \mathbf{C}_a^b is the transformation matrix, called the direct cosine matrix (DCM).

There are two properties used in dynamic equations and described as:

A.

The time derivative of the transformation matrix is given by:

$$\dot{\mathbf{C}}_a^b = \lim_{\Delta t \rightarrow 0} \frac{\Delta \mathbf{C}_a^b}{\Delta t} = \lim_{\Delta t \rightarrow 0} \frac{\mathbf{C}_a^b(t + \Delta t) - \mathbf{C}_a^b(t)}{\Delta t} \quad (3.3.2)$$

$$\mathbf{C}_a^b(t + \Delta t) = \mathbf{C}_a^b(t) \cdot (\mathbf{I} + \Delta \theta^a) \quad (3.3.3)$$

where $(\mathbf{I} + \Delta \theta^a)$ is the small angle transformation relating the a frame at time t to the rotated a frame at time $t + \Delta t$.

Then substituting (3.3.3) into (3.3.2)

$$\dot{\mathbf{C}}_a^b = \mathbf{C}_a^b(t) \lim_{\Delta t \rightarrow 0} \frac{\Delta \theta^a}{\Delta t} \quad (3.3.4)$$

define

$$\lim_{\Delta t \rightarrow 0} \frac{\Delta \theta^a}{\Delta t} = \boldsymbol{\Omega}_{ba}^a$$

where $\boldsymbol{\Omega}_{ba}^a$ is the angular velocity of the a frame w.r.t. the b frame, with coordinates in the a frame.

Consequently

$$\dot{\mathbf{C}}_a^b = \mathbf{C}_a^b \boldsymbol{\Omega}_{ba}^a \quad (3.3.5)$$

where $\boldsymbol{\Omega}_{ba}^a$ denotes a skew-symmetric matrix with elements from ω_{ba}^a .

$$\Omega_{ba}^a \equiv [\omega_{ba}^a \times] = \begin{bmatrix} 0 & -\omega_z & \omega_y \\ \omega_z & 0 & -\omega_x \\ -\omega_y & \omega_x & 0 \end{bmatrix} \quad (3.3.6)$$

B.

Since the columns of C_a^b are mutually orthogonal, as are the rows. Therefore the matrix C_a^b is an orthogonal matrix, i.e.

$$C_b^a \equiv (C_a^b)^{-1} = (C_a^b)^T \quad (3.3.7)$$

For any 3-by-3 matrix, A^a , under an orthogonal frame transformation can be derived as follows. Let $r^a = A^a r^a$. From the transformation between coordinates described in (3.3.1) and the property derived in (3.3.7), we have

$$r^b = C_a^b A^a C_b^a r^b \quad (3.3.8)$$

From (3.3.8), it follows that

$$A^b = C_a^b A^a C_b^a \quad (3.3.9)$$

These two properties would be useful in deriving dynamic equation. Furthermore, the next section would start the derivation of velocity dynamic equation.

3.3.2 Velocity Dynamic Equation

After the necessary properties (3.3.5) and (3.3.9) are given, the derivation of the velocity dynamic equation could be started from measuring the specific force in motions based on the Newton's law.

First, let's consider the force exerted on the system in the inertial coordinate

frame, say i frame [9, 10], which is obtained as

$$\mathbf{f}^i = \ddot{\mathbf{r}}^i - \mathbf{G}^i \quad (3.3.10)$$

where \mathbf{r}^i and \mathbf{G}^i represent the positional vector and gravitational acceleration at the system, respectively. Now define the position vector and velocity vector in the navigation coordinate frame, say n frame, as $\mathbf{r}^n = [r_N \ r_E \ r_D]$ and $\mathbf{v}^n = [v_N \ v_E \ v_D]$. Further applying the transformation between two different coordinates shown as (3.3.1), we have

$$\mathbf{r}^e = \mathbf{C}_i^e \mathbf{r}^i \quad (3.3.11)$$

$$\mathbf{v}^n = \mathbf{C}_e^n \dot{\mathbf{r}}^e \quad (3.3.12)$$

where the super indices e and n denote the Earth coordinate and navigation coordinate.

Substituting (3.3.11) into (3.3.12) leads to

$$\begin{aligned} \mathbf{v}^n &= \mathbf{C}_e^n (\mathbf{C}_i^e \dot{\mathbf{r}}^i + \dot{\mathbf{C}}_i^e \mathbf{r}^i) \\ &= \mathbf{C}_e^n (\mathbf{C}_i^e \dot{\mathbf{r}}^i + \mathbf{C}_i^e \boldsymbol{\Omega}_{ei}^i \mathbf{r}^i) \\ &= \mathbf{C}_i^n (\dot{\mathbf{r}}^i + \boldsymbol{\Omega}_{ei}^i \mathbf{r}^i) \\ &= \mathbf{C}_i^n (\dot{\mathbf{r}}^i - \boldsymbol{\Omega}_{ie}^i \mathbf{r}^i) \end{aligned} \quad (3.3.13)$$

The time derivative of (3.3.13) is given by

$$\begin{aligned} \dot{\mathbf{v}}^n &= \mathbf{C}_i^n \ddot{\mathbf{r}}^i + \dot{\mathbf{C}}_i^n \dot{\mathbf{r}}^i - \dot{\mathbf{C}}_i^n \boldsymbol{\Omega}_{ie}^i \mathbf{r}^i - \mathbf{C}_i^n \dot{\boldsymbol{\Omega}}_{ie}^i \mathbf{r}^i - \mathbf{C}_i^n \boldsymbol{\Omega}_{ie}^i \dot{\mathbf{r}}^i - \mathbf{C}_i^n \dot{\boldsymbol{\Omega}}_{ie}^i \mathbf{r}^i \\ &= \mathbf{C}_i^n [\ddot{\mathbf{r}}^i - (\boldsymbol{\Omega}_{ie}^i + \boldsymbol{\Omega}_{in}^i) \dot{\mathbf{r}}^i + \boldsymbol{\Omega}_{in}^i \boldsymbol{\Omega}_{ie}^i \mathbf{r}^i] - \mathbf{C}_i^n \dot{\boldsymbol{\Omega}}_{ie}^i \mathbf{r}^i \end{aligned} \quad (3.3.14)$$

Since $\boldsymbol{\Omega}_{ie}^i = \mathbf{C}_n^i \boldsymbol{\Omega}_{ie}^n \mathbf{C}_i^n$, $\boldsymbol{\Omega}_{in}^i = \mathbf{C}_n^i \boldsymbol{\Omega}_{in}^n \mathbf{C}_i^n$ and assume $\dot{\boldsymbol{\Omega}}_{ie}^i = 0$, it is attained that

$$\begin{aligned} \dot{\mathbf{v}}^n &= \mathbf{C}_i^n [\ddot{\mathbf{r}}^i - \mathbf{C}_n^i (\boldsymbol{\Omega}_{ie}^n + \boldsymbol{\Omega}_{in}^n) \mathbf{C}_i^n \dot{\mathbf{r}}^i + \mathbf{C}_n^i \boldsymbol{\Omega}_{in}^n \mathbf{C}_i^n \mathbf{C}_n^i \boldsymbol{\Omega}_{ie}^n \mathbf{C}_i^n \mathbf{r}^i] \\ &= \mathbf{C}_i^n \ddot{\mathbf{r}}^i - (\boldsymbol{\Omega}_{ie}^n + \boldsymbol{\Omega}_{in}^n) \mathbf{C}_i^n \dot{\mathbf{r}}^i + \boldsymbol{\Omega}_{in}^n \boldsymbol{\Omega}_{ie}^n \mathbf{C}_i^n \mathbf{r}^i \end{aligned}$$

From (3.3.13) and (3.3.1), we have

$$\begin{aligned}
\dot{\mathbf{v}}^n &= \mathbf{C}_i^n \ddot{\mathbf{r}}^i - (\Omega_{ie}^n + \Omega_{in}^n) (\mathbf{v}^n + \mathbf{C}_i^n \Omega_{ie}^i \mathbf{r}^i) + \Omega_{in}^n \Omega_{ie}^n \mathbf{r}^n \\
&= \mathbf{C}_i^n \ddot{\mathbf{r}}^i - (\Omega_{ie}^n + \Omega_{in}^n) \mathbf{v}^n - (\Omega_{ie}^n + \Omega_{in}^n) (\mathbf{C}_i^n \mathbf{C}_n^i \Omega_{ie}^n \mathbf{C}_i^n \mathbf{r}^i) + \Omega_{in}^n \Omega_{ie}^n \mathbf{r}^n \\
&= \mathbf{C}_i^n \ddot{\mathbf{r}}^i - (\Omega_{ie}^n + \Omega_{in}^n) \mathbf{v}^n - (\Omega_{ie}^n + \Omega_{in}^n) \Omega_{ie}^n \mathbf{r}^n + \Omega_{in}^n \Omega_{ie}^n \mathbf{r}^n \\
&= \mathbf{C}_i^n \ddot{\mathbf{r}}^i - (\Omega_{ie}^n + \Omega_{in}^n) \mathbf{v}^n - \Omega_{ie}^n \Omega_{ie}^n \mathbf{r}^n
\end{aligned} \tag{3.3.15}$$

Pre-multiplying (3.3.10) by \mathbf{C}_i^n yields

$$\mathbf{f}^n = \mathbf{C}_i^n \ddot{\mathbf{r}}^i - \mathbf{G}^n \tag{3.3.16}$$

Substituting (3.3.16) into (3.3.15) shows that

$$\dot{\mathbf{v}}^n + (\Omega_{ie}^n + \Omega_{in}^n) \mathbf{v}^n = \mathbf{f}^n + (\mathbf{G}^n - \Omega_{ie}^n \Omega_{ie}^n \mathbf{r}^n) \tag{3.3.17}$$

where $\Omega_{ie}^n \Omega_{ie}^n \mathbf{r}^n$ represents the centripetal acceleration.

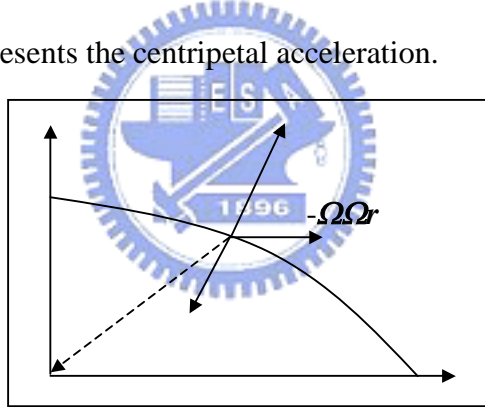


Figure 3.8 Gravitational acceleration vector in the navigation frame

Define the gravity vector in the n frame as

$$\mathbf{g}^n = \mathbf{G}^n - \Omega_{ie}^n \Omega_{ie}^n \mathbf{r}^n \tag{3.3.18}$$

then (3.3.17) would be rewritten into

$$\dot{\mathbf{v}}^n + (\Omega_{ie}^n + \Omega_{in}^n) \mathbf{v}^n = \mathbf{f}^n + \mathbf{g}^n \tag{3.3.19}$$

where $\Omega_{ie}^n \mathbf{v}^n = \omega_{ie}^n \times \mathbf{v}^n$, also note that ω_{ie}^n , ω_{in}^n represent the Earth rate vector and the angular rate respectively in the n frame relative to i frame. Traditionally,

$$\Omega_{ie}^n = \omega_{ie}^n \times = \begin{bmatrix} \omega_e \cos L \\ 0 \\ -\omega_e \sin L \end{bmatrix} \times = \begin{bmatrix} 0 & \omega_e \sin L & 0 \\ -\omega_e \sin L & 0 & -\omega_e \cos L \\ 0 & \omega_e \cos L & 0 \end{bmatrix}$$

$$\Omega_{in}^n = \omega_{in}^n \times = \begin{bmatrix} (\omega_e + \dot{l}) \cos L \\ \dot{L} \\ -(\omega_e + \dot{l}) \sin L \end{bmatrix} \times = \begin{bmatrix} 0 & (\omega_e + \dot{l}) \sin L & \dot{L} \\ -(\omega_e + \dot{l}) \sin L & 0 & -(\omega_e + \dot{l}) \cos L \\ -\dot{L} & (\omega_e + \dot{l}) \cos L & 0 \end{bmatrix}$$

Hence, (3.3.19) could be expressed as the following the state-space form:

$$\begin{bmatrix} \dot{v}_N^n \\ \dot{v}_E^n \\ \dot{v}_D^n \end{bmatrix} = \begin{bmatrix} 0 & -(2\omega_e + \dot{l}) \sin L & \dot{L} \\ (2\omega_e + \dot{l}) \sin L & 0 & (2\omega_e + \dot{l}) \cos L \\ -\dot{L} & -(2\omega_e + \dot{l}) \cos L & 0 \end{bmatrix} \begin{bmatrix} v_N^n \\ v_E^n \\ v_D^n \end{bmatrix} + \begin{bmatrix} f_N^n \\ f_E^n \\ f_D^n \end{bmatrix} + \begin{bmatrix} 0 \\ 0 \\ g^n \end{bmatrix} \quad (3.3.20)$$

Consequently, (3.3.19~20) are the velocity dynamic equations useful for inertial navigation and autonomous control of vehicle.

In addition, the relation between n and geodetic frames is shown as

$$\begin{bmatrix} v_N^n \\ v_E^n \\ v_D^n \end{bmatrix} = \begin{bmatrix} \rho_M + h & 0 & 0 \\ 0 & (\rho_P + h) \cos L & 0 \\ 0 & 0 & -1 \end{bmatrix} \begin{bmatrix} \dot{L} \\ \dot{l} \\ \dot{h} \end{bmatrix} \quad (3.3.21)$$

or

$$\begin{bmatrix} \dot{L} \\ \dot{l} \\ \dot{h} \end{bmatrix} = \begin{bmatrix} \frac{1}{\rho_M + h} & 0 & 0 \\ 0 & \frac{1}{(\rho_P + h) \cos L} & 0 \\ 0 & 0 & -1 \end{bmatrix} \begin{bmatrix} v_N^n \\ v_E^n \\ v_D^n \end{bmatrix} \quad (3.3.22)$$

where

$$\rho_M \cong a \left[1 + \frac{e^2}{2} (e^2 \cdot \sin^2 L - 1) \right] \approx R$$

$$\rho_P \cong a \left[1 + \frac{e^2}{2} \cdot \sin^2 L \right] \approx R$$

With the dynamic equation in (3.3.20) and the relations in (3.3.21-22), the INS dynamic equations are more complete. In next section, the INS error model would be introduced to realize how the errors affect the INS system performance.

3.4 INS Error Model

The inertial navigation system is a rather complex instrument whose components would affect the system errors due to initial random errors and modeling errors. Therefore, in order to understand the influence of the system errors in navigation solution, it is important to develop the dynamic and stochastic models for these system errors.

3.4.1 Error Model

How the sensor errors affect the position and velocity is described by the dynamic error model which be derived by applying a differential operator δ to the dynamic navigation equations. That is, the variables of the navigation equations are perturbed differentially. There are two approaches generally employed to derive dynamic error model: perturbation approach and psi-angle approach [4].

First, from (3.3.22) the use of perturbation approach would give the dynamic error model as

$$\begin{bmatrix} \delta \dot{L} \\ \delta \dot{i} \\ \delta \dot{h} \end{bmatrix} = \begin{bmatrix} \frac{1}{\rho_M + h} & 0 & 0 \\ 0 & \frac{1}{(\rho_P + h) \cos L} & 0 \\ 0 & 0 & -1 \end{bmatrix} \begin{bmatrix} \delta v_N \\ \delta v_E \\ \delta v_D \end{bmatrix} + \begin{bmatrix} -\frac{\dot{L}}{\rho_M + h} \\ \dot{i} \\ \frac{0}{(\rho_P + h)} \end{bmatrix} \delta h + \begin{bmatrix} 0 \\ i \tan(L) \delta L \\ 0 \end{bmatrix} \quad (3.4.1)$$

In this thesis, the psi-angle approach is adopted and the dynamic error model is

represented as [4]

$$\delta \dot{\mathbf{r}}^n + \boldsymbol{\rho} \times \delta \mathbf{r}^n = \delta \mathbf{v}^n \quad (3.4.2)$$

$$\delta \dot{\mathbf{v}}^n + (\boldsymbol{\omega}_{ie}^n + \boldsymbol{\omega}_{in}^n) \times \delta \mathbf{v}^n = \nabla - \delta \boldsymbol{\psi} \times \mathbf{f}^n + \Delta \mathbf{g}^n \quad (3.4.3)$$

$$\delta \dot{\boldsymbol{\psi}} + \boldsymbol{\omega}_{in}^n \times \delta \boldsymbol{\psi} = \boldsymbol{\varepsilon} \quad (3.4.4)$$

where

$\delta \mathbf{v}$: velocity error vector.

$\delta \mathbf{r}$: position error vector.

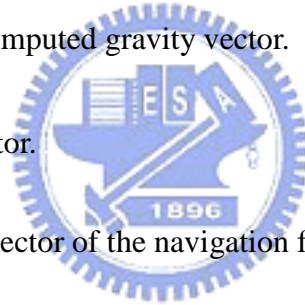
$\delta \boldsymbol{\psi}$: attitude error vector.

∇ : accelerometer error vector.

$\Delta \mathbf{g}$: error in the computed gravity vector.

$\boldsymbol{\varepsilon}$: gyro drift vector.

$\boldsymbol{\rho}$: rotation rate vector of the navigation frame w.r.t. the Earth.



The state space form of (3.3.2~4) is given as

$$\delta \dot{\mathbf{X}}_I = \mathbf{A}_I \delta \mathbf{X}_I + \mathbf{B}_I \quad (3.4.5)$$

where

$$\delta \mathbf{X}_I = [\delta r_N \quad \delta r_E \quad \delta r_D \quad \delta v_N \quad \delta v_E \quad \delta v_D \quad \delta \psi_N \quad \delta \psi_E \quad \delta \psi_D]^T$$

$$\mathbf{A}_I = \begin{bmatrix} \mathbf{A}_{11} & \mathbf{I}_{3 \times 3} & \mathbf{0}_{3 \times 3} \\ \mathbf{A}_{21} & \mathbf{A}_{22} & \mathbf{A}_{23} \\ \mathbf{0}_{3 \times 3} & \mathbf{0}_{3 \times 3} & \mathbf{A}_{33} \end{bmatrix}_{9 \times 9}$$

$$\mathbf{A}_{11} = \begin{bmatrix} 0 & -\dot{L} \sin L & \dot{L} \\ \dot{L} \sin L & 0 & \dot{L} \cos L \\ -\dot{L} & -\dot{L} \cos L & 0 \end{bmatrix}$$

$$\mathbf{A}_{21} = \begin{bmatrix} -g/R & 0 & 0 \\ 0 & -g/R & 0 \\ 0 & 0 & 2g/R \end{bmatrix}$$

$$\mathbf{A}_{22} = \begin{bmatrix} 0 & -(2\omega_{ie}^n + \dot{l})\sin L & \dot{L} \\ (2\omega_{ie}^n + \dot{l})\sin L & 0 & (2\omega_{ie}^n + \dot{l})\cos L \\ -\dot{L} & -(2\omega_{ie}^n + \dot{l})\cos L & 0 \end{bmatrix}$$

$$\mathbf{A}_{23} = \begin{bmatrix} 0 & -f_D & f_E \\ f_D & 0 & -f_N \\ -f_E & f_N & 0 \end{bmatrix}$$

$$\mathbf{A}_{33} = \begin{bmatrix} 0 & -(\omega_{ie}^n + \dot{l})\sin L & \dot{L} \\ (\omega_{ie}^n + \dot{l})\sin L & 0 & (\omega_{ie}^n + \dot{l})\cos L \\ -\dot{L} & -(\omega_{ie}^n + \dot{l})\cos L & 0 \end{bmatrix}$$

$$\mathbf{B}_I = [0 \quad 0 \quad 0 \quad \nabla_N \quad \nabla_E \quad \nabla_D \quad \varepsilon_N \quad \varepsilon_E \quad \varepsilon_D]^T$$

Actually, there exist stochastic characteristics in sensor. Therefore, in the following section, the stochastic model of sensors will be derived and expounded.

3.4.2 Error Sources

The major error sources of INS are gyro and accelerometer, and furthermore their bias and scale factor error are not always white noise. In this section, the principle work is to discuss these sources and model these errors, so that the INS error model would be completely expounded. The discussion can be separated into two parts: gyro and accelerometer [19~21].

In general, gyro has four types of error, such as random bias B_g , scale factor SF_g , random drift ε_g , and random noise w_g . The instrument specification can be described as:

$$\dot{\psi} = B_g + \varepsilon_g + w_g + SF_g \times \omega \quad (3.4.6)$$

where $\dot{\psi}$ represents the output of the gyro

ω represents the angular rate of the vehicle.

These four types of error can be modeled as:

$$\dot{B}_g = 0$$

$$SF_g = 0$$

$$E\{\varepsilon_g\} = 0$$

$$E\{\varepsilon_g(t) \cdot \varepsilon_g(\tau)\} = \sigma_{\varepsilon_g}^2 \delta(t - \tau)$$

$$\dot{w}_g = -w_g/\tau_g + w_{gn}$$

where τ_g is the correlation time of random noise w_g .

$$E\{w_{gn}\} = 0$$

$$E\{w_{gn}(t) \cdot w_{gn}(\tau)\} = \sigma_{w_{gn}}^2 \delta(t - \tau)$$

$$Q_{gn} = \sqrt{2\sigma_{gn}^2/\tau_g} \text{ represents the power spectrum of } w_{gn}$$

Therefore, the gyro errors can be modeled as:

$$\delta \dot{X}_g = A_g \delta X_g + w_1 \quad (3.4.7)$$

where $\delta X_g = [w_{gN} \quad w_{gE} \quad w_{gD} \quad B_{gN} \quad B_{gE} \quad B_{gD} \quad SF_{gN} \quad SF_{gE} \quad SF_{gD}]^T$

$$A_g = \left[\begin{array}{ccc|c} -1/\tau_{gN} & 0 & 0 & \mathbf{0}_{3 \times 6} \\ 0 & -1/\tau_{gE} & 0 & \\ 0 & 0 & -1/\tau_{gD} & \\ \hline \mathbf{0}_{6 \times 3} & & & \mathbf{0}_{6 \times 6} \end{array} \right]$$

$$w_1 = [w_{gnN} \quad w_{gnE} \quad w_{gnD} \quad 0 \quad 0 \quad 0 \quad 0 \quad 0 \quad 0]^T$$

As the same discussion above, the instrument specification of accelerometer can be expressed as

$$\dot{v} = \Delta + B_a + SF_a \times f \quad (3.4.8)$$

where \dot{v} represents the output of accelerometer

Δ represents the random drift

B_a represents the random bias

SF_a represents the scale factor

f represents the acceleration of vehicle

The accelerometer errors can be modeled as

$$SF_a \dot{=} 0$$

$$E\{\Delta\} = 0$$

$$E\{\Delta(t) \cdot \Delta(\tau)\} = \sigma_\Delta^2 \delta(t - \tau)$$

$$\dot{B}_a = -B_a/\tau_a + w_a$$

where τ_a represents the correlation time of random bias

$$E\{w_a\} = 0$$

$$E\{w_a(t) \cdot w_a(\tau)\} = \sigma_{w_a}^2 \delta(t - \tau)$$

$Q_a = \sqrt{2\sigma_a^2/\tau_a}$ represents the power spectrum of w_a

Thus, the accelerometer errors can be modeled as:

$$\delta \dot{X}_a = A_a \delta X_a + w_2 \quad (3.4.9)$$

where $\delta X_a = [B_{aN} \quad B_{aE} \quad B_{aD} \quad SF_{aN} \quad SF_{aE} \quad SF_{aD}]^T$

$$A_a = \begin{bmatrix} -1/\tau_{aN} & 0 & 0 & \vdots & \vdots & \vdots \\ 0 & -1/\tau_{aE} & 0 & \mathbf{0}_{3 \times 3} & \vdots & \vdots \\ 0 & 0 & -1/\tau_{aD} & \vdots & \vdots & \vdots \\ \hline \vdots & \mathbf{0}_{3 \times 3} & \vdots & \mathbf{0}_{3 \times 3} & \vdots & \vdots \end{bmatrix}$$

$$w_2 = [w_{aN} \quad w_{aE} \quad w_{aD} \quad 0 \quad 0 \quad 0]^T$$

With the discussion of errors in IMU (3.4.7~9), the dynamic error model mentioned in

(3.4.5) would be extended to 24 state variables and shown as

$$\delta \dot{X} = A \delta X + B \quad (3.4.10)$$

where $\delta X = [\delta r \quad \delta v \quad \delta \psi \quad w_g \quad B_g \quad SF_g \quad B_a \quad SF_a]^T$

$$A = \begin{bmatrix} \mathbf{A}_{I_{9 \times 9}} & \mathbf{0}_{3 \times 3} & \mathbf{0}_{3 \times 3} & \mathbf{0}_{3 \times 3} & \mathbf{0}_{3 \times 3} & \mathbf{0}_{3 \times 3} \\ \mathbf{0}_{3 \times 3} & \mathbf{0}_{3 \times 3} & \mathbf{0}_{3 \times 3} & \mathbf{I}_{3 \times 3} & \mathbf{f}_{3 \times 3} & \mathbf{0}_{3 \times 3} \\ \mathbf{I}_{3 \times 3} & \mathbf{I}_{3 \times 3} & \omega_{3 \times 3} & \mathbf{0}_{3 \times 3} & \mathbf{0}_{3 \times 3} & \mathbf{0}_{3 \times 3} \\ \hline \mathbf{0}_{9 \times 9} & \mathbf{A}_{g_{9 \times 9}} & \mathbf{0}_{9 \times 6} & \mathbf{0}_{9 \times 3} & \mathbf{0}_{9 \times 3} & \mathbf{0}_{9 \times 3} \\ \hline \mathbf{0}_{6 \times 9} & \mathbf{0}_{6 \times 9} & \mathbf{0}_{6 \times 6} & \mathbf{0}_{6 \times 3} & \mathbf{A}_{a_{6 \times 6}} & \mathbf{0}_{6 \times 3} \end{bmatrix}_{24 \times 24}$$

$$\mathbf{B} = \left[\mathbf{0} \mid \Delta \mid \varepsilon_g \mid \mathbf{w}_{gn} \mid \mathbf{0} \mid \mathbf{0} \mid \mathbf{w}_a \mid \mathbf{0} \right]_{1 \times 24}^T$$

Consequently, this INS error model composed of dynamic and stochastic models describes how the dynamics equation and sensor errors propagate through the system into navigation errors.

3.4.3 The Reduced Error Model

In this subsection, the reduced error model for this system will be described. From the error model in (3.4.10), the state variables $\delta\mathbf{X}$ of the model can be reduced as to the following form.

$$\delta\dot{\mathbf{X}}' = \mathbf{A}' \delta\mathbf{X}' + \mathbf{B}' \quad (3.4.11)$$

where

$$\delta\mathbf{X}' = \left[\delta r_N \quad \delta r_E \quad \delta V_N \quad \delta V_E \quad \delta \psi \quad \mathbf{w}_g \quad \mathbf{B}_a \quad \mathbf{B}_g \quad \mathbf{SF}_a \quad \mathbf{SF}_g \right]^T$$

$$\mathbf{A}' = \begin{bmatrix} 0 & -\dot{L} \sin L & 1 & 0 & 0 & 0 & 0 & 0 & 0 & 0 & 0 \\ \dot{L} \sin L & 0 & 0 & 1 & 0 & 0 & 0 & 0 & 0 & 0 & 0 \\ -g/R & 0 & 0 & -(2\omega_{ie}^n + \dot{L}) \sin L & f_E & 0 & \cos \psi & 0 & f_N & 0 \\ 0 & -g/R & (2\omega_{ie}^n + \dot{L}) \sin L & 0 & -f_N & 0 & \sin \psi & 0 & f_E & 0 \\ 0 & 0 & 0 & 0 & 0 & 0 & 1 & 0 & 1 & 0 & \omega \\ \hline 0 & 0 & 0 & 0 & 0 & 0 & -1/\tau_g & 0 & 0 & 0 & 0 \\ 0 & 0 & 0 & 0 & 0 & 0 & 0 & -1/\tau_a & 0 & 0 & 0 \\ 0 & 0 & 0 & 0 & 0 & 0 & 0 & 0 & 0 & 0 & 0 \\ 0 & 0 & 0 & 0 & 0 & 0 & 0 & 0 & 0 & 0 & 0 \\ 0 & 0 & 0 & 0 & 0 & 0 & 0 & 0 & 0 & 0 & 0 \end{bmatrix}_{10 \times 10}$$

where \mathbf{B}' = the input noise vector.

$$\mathbf{B}' = \left[0 \quad 0 \quad \Delta_N \quad \Delta_E \quad \varepsilon_g \quad \mathbf{w}_{gn} \quad \mathbf{w}_a \quad 0 \quad 0 \quad 0 \right]^T$$

Which has zero mean and with covariance as

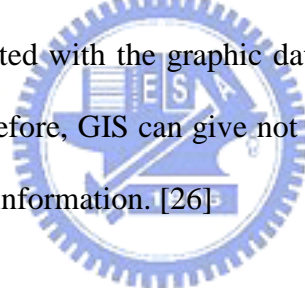
$$\mathbf{Q} = \text{diag} \left[0 \quad 0 \quad \sigma_{\Delta_N}^2 \quad \sigma_{\Delta_E}^2 \quad \sigma_{\varepsilon_g}^2 \quad \sigma_{\mathbf{w}_{gn}}^2 \quad \sigma_{\mathbf{w}_y}^2 \quad 0 \quad 0 \quad 0 \right]$$

This reduced form is used in Kalman filter, and next; the general form of Kalman filter will be discussed.

Chapter 4 Geographic Information System

4.1 Introduction

The Federal Interagency Coordinating Committee defined the term *Geographic Information System* in the following manner: “ A system including computer hardware, software, and procedure, which is designed to support the capture, management, manipulation, analysis, modeling, and display of spatially referenced data for solving complex planning and management problems” in 1988. Such a system is an electronic spreadsheet coupled with powerful graphic-manipulation and display capabilities. In general, a geographic information system (GIS) combines graphic system and data processing system to manage the graphic data, characters, numeral data, and attribute data. Attribute data is associated with the graphic data and provide more descriptive information about them. Therefore, GIS can give not only the information of the data element itself, but the nearby information. [26]



4.2 Reference Ellipsoids and Projection

This section would describe the reference ellipsoids, which would be used in projection and coordinate transformation. Ellipsoidal models define an ellipsoid with an equatorial radius (semi-major axis) and a polar radius (semi-minor axis) that is shown as figure 4.1. There are three kinds of reference ellipsoid parameters shown as table 4.1. Reference ellipsoids used with different nations and agencies are shown as table 4.2.

To transform three-dimensional space onto two-dimensional map is called “Projection”. Projection formulas convert a geographical location on sphere or spheroid to a representative location on flat surface. There are three commonly

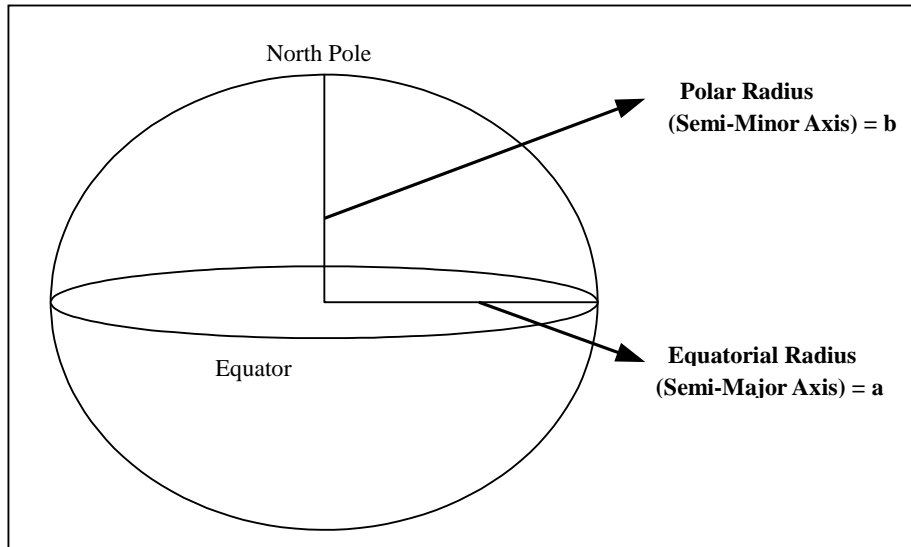


Figure 4.1 Semi-major axis and semi-minor axis

Table 4.1 Ellipsoidal Parameters

Ellipsoid Parameters	Functions
f (Flattening)	$f = \frac{a-b}{a}$
e^2 (First Eccentricity Squared)	$e^2 = \frac{a^2 - b^2}{a^2} = 2f - f^2$
e'^2 (Second Eccentricity Squared)	$e'^2 = \frac{a^2 - b^2}{b^2}$

Table 4.2 Selected reference ellipsoids

Ellipse	Semi-Major Axis (Meters)	1/Flattening
G R S 1967	6378160.0	298.247167427
G R S 1975	6378140.0	298.257
G R S 1980	6378137.0	298.257222101
Hough 1956	6378270.0	297.0
International	6378388.0	297.0
Krassovsky 1940	6378245.0	298.3
South American 1969	6378160.0	298.25
WGS 60	6378165.0	298.3
WGS 66	6378145.0	298.25
WGS 72	6378135.0	298.26
WGS 84	6378137.0	298.257223563

projections, azimuthal projection, cylindrical projection, and conical projection shown as figure 4.2. Azimuthal projection can be classified into three types based on the difference of the projected origin shown as figure 3.6.

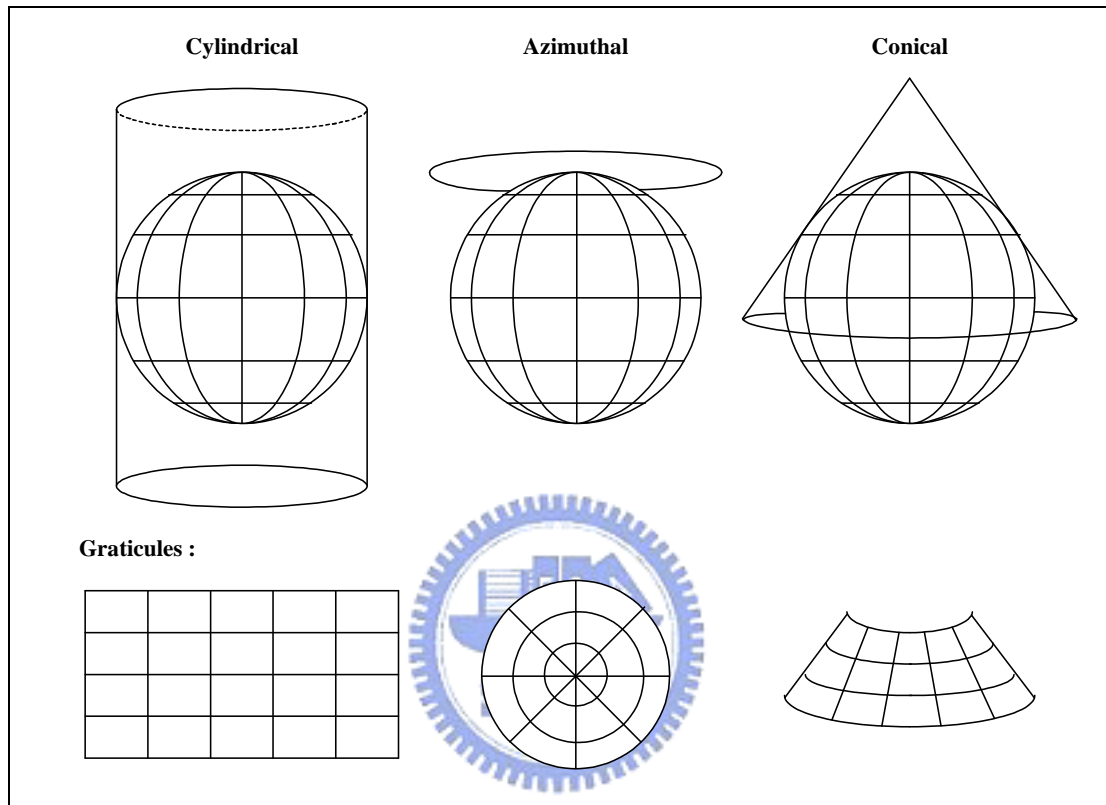
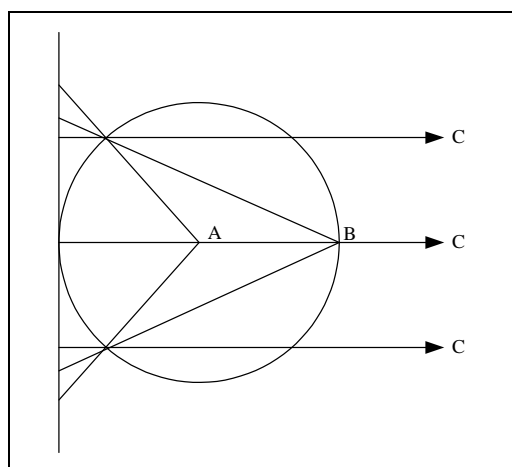


Figure 4.2 Projections and the appearance of the Graticules



- A: Gnomonic (from center of the Earth)
- B: Stereographic (from a diameter's distance)
- C: Orthographic (from infinity)

Figure 4.3 Azimuthal projection

4.3 Taiwan Coordinates

The conventional geodetic datum used in Taiwan was based on the geodetic observations carried out in 1978, and the reference ellipsoid was the Geodetic Reference System 1967 (GRS67). The origin point of this datum locates at the Hu-Tzu-Shan astronomic station. The coordinates, which includes the latitude and longitude based on the GRS67, grid coordinate based on 2°-Zone Transverse Mercator (TM) projection, and the height is above the mean sea level. The set of coordinates adopted in Taiwan was called the Hu-Tzu-Shan coordinate system, and also named the TWD67 (Taiwan Geodetic Datum based on the GRS67). [27]

The recommendations made by the IERS (International Earth Rotation Service) also encourage national agencies to establish their precise national datum based on the ITRF (International Terrestrial Reference Frame). This datum would be linked into regional or continental solutions and employed for many international applications. Thus, a geodetic ellipsoid, GRS80, was adopted with the new national coordinate system called the TWD97 that also employs the Transverse Mercator. Table 4.3 shows the parameters of TWD67TM2 and TWD97TM2 coordinates in Taiwan. The grid coordinate is calculated with a 2-degree zone and 121° E and 119° E. Furthermore, the western offset of the transverse axis is 250,000 m and the scale ratio is 0.9999, where the scale ratio is defined as:

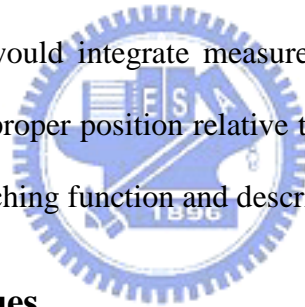
$$\text{Scale ratio} = \text{actual map scale} / \text{nominal scale}$$

Table 4.3 Taiwan coordinates

Coordinates	Reference Ellipsoids	Semi-Major Axis	1/Flattening	Central Meridians	Western Offset	Scale Ratio
TWD67TM2	GRS67	6378160.0	298.247167427	121°E,119°E	250,000 m	0.9999
TWD97TM2	GRS80	6378137.0	298.257222101	121°E,119°E	250,000 m	0.9999

4.4 Map Matching Algorithm

The purpose of the map-matching algorithm is to locate the position of the vehicle on the map. Since the GPS satellite signal has errors and noise due to the tropospheric and ionospheric propagation delays, and GIS database is more accurate. Therefore, a map-matching method using a digital map is a useful approach to correct these errors. Furthermore, the fact that “ A vehicle moves always on a road network. ” makes the utilization of the map information more effective. With the assumption that land-vehicle almost run on roads, most of vehicle navigation systems translate the GPS position onto a road, and the position errors can be eliminated if the road where the car locates can be found. In other words, the map-matching problem can be defined as the identification problem of the road where the car locates. Furthermore, the map-matching function would integrate measured position and the digital map data to locate the vehicle on proper position relative to digital map. There are several criterion used in the map-matching function and described in the following sections.



4.4.1 Map Matching Issues

There are three issues that would be discussed in the map-matching algorithm and presented as the following description. Projected error is defined as the distance between the measured position obtained from the GPS/INS and its projected position on the road shown as figure 4.4. Therefore, the first issue of the map-matching algorithm is that the projected error must be small, so that the correct located road would be found. The dot-product implies the similarity between the shape of the road and the trajectory of the vehicle shown as figure 4.5. Thus, the second issue of map-matching algorithm is that the dot-product value should be big, so that the vehicle would be matched to the correct road due to the fact that the trajectory is similar to the shape of road. The definition of the moving distance is the distance

between the present vehicle position and the previous vehicle position shown as figure 4.6. Accordingly, the third issue is that the difference between the moving distance and the projected moving distance should be small. Consequently, these three issues would be useful to decide which road the vehicle runs. Next section would discuss the map-matching structure and give the flowchart. [11]

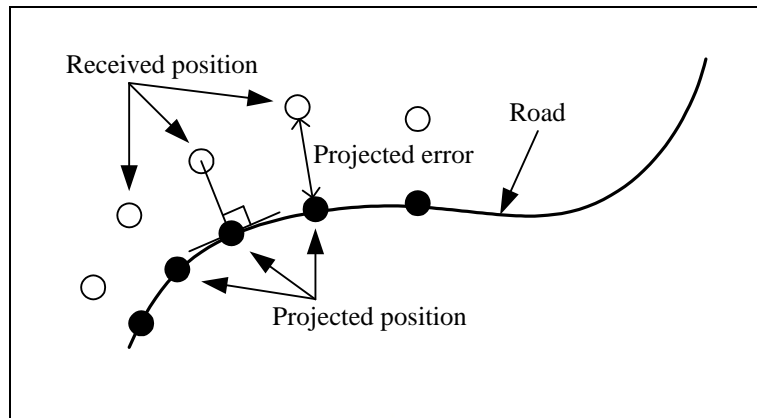


Figure 4.4 Projected errors

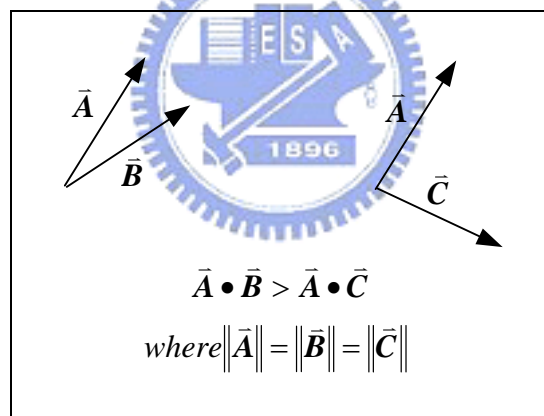


Figure 4.5 Dot-product

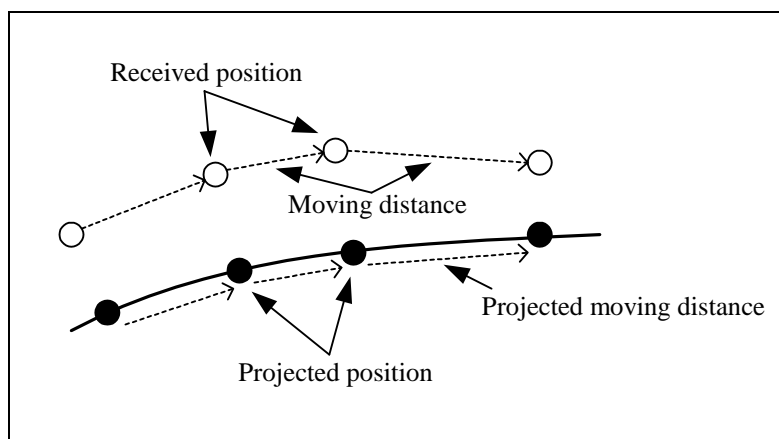


Figure 4.6 Moving distance

4.4.2 Map Matching Structure

In the map-matching structure, three modes are used and they are initial mode, searching mode, and tracking mode. In the initial mode, only the projected error measurement is used, and the first issue would decide the closest road and the closest point. As the vehicle starts to run, the navigation system would detect how many nodes, which are the junctions of two or more roads, are near the vehicle. If there were nodes nearby, the mode would be changed to the searching mode. As the matched road and matched point are decided, the mode would back to the nodes nearby decision. If there is no node nearby, the mode would be changed to the tracking mode, and that means the vehicle position approaches only one road. Then, the projection method would be employed to decide the projected point of the initial road or the previous matched road. Furthermore, the mode would also back to the nodes nearby decision after the projected point is calculated. The complete map-matching flowchart is shown in figure 4.7 and the detail procedure of the map-matching structure is presented in the next four sections.

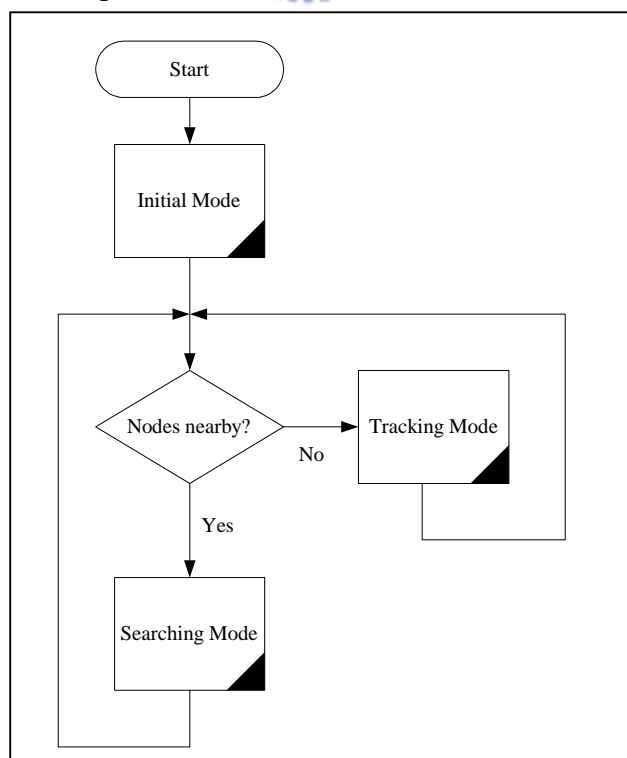


Figure 4.7 Map matching flowchart

4.4.3 Initial Mode

The projected error and first issue are used to determine the closest road and the closest point in the initial mode. The initial mode includes three steps:

1. Search the roads in the range of 150 m.
2. Find the closest road.
3. Find the closest point on the closest road.

Figure 4.8 shows that the navigation system would search the roads around the measured position and find the closest road and point.

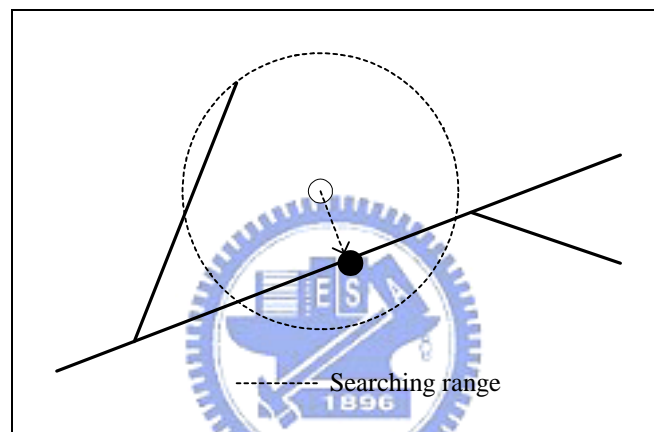


Figure 4.8 Initial mode

4.4.4 Nodes Nearby Detection and Searching Mode

The node nearby detection is always applied when a new measured position is obtained. The node nearby detection is used to judge that the next mode is the searching mode if there are nodes nearby or the tracking mode if there is no node nearby. In addition, the searching range of this detection is 20 m.

In searching mode, these three issues have different processing priorities respectively. The projected error has the highest priority, and the moving distance has the lowest priority. As the GPS/INS position is obtained in the searching mode, the system would search the candidate roads with searching range of 20 m. If there is only

one candidate road, the projection method is adopted only. If there are more than one candidate roads, the dot-product operation is employed. From the second issue of the map-matching algorithm, the road that has the biggest dot-product value is the matched road. However, if the difference between the two biggest dot-product values were smaller than 0.1, the moving distance judgment would be applied to decide the matched road. The complete flowchart of the searching mode is shown in figure 4.9.

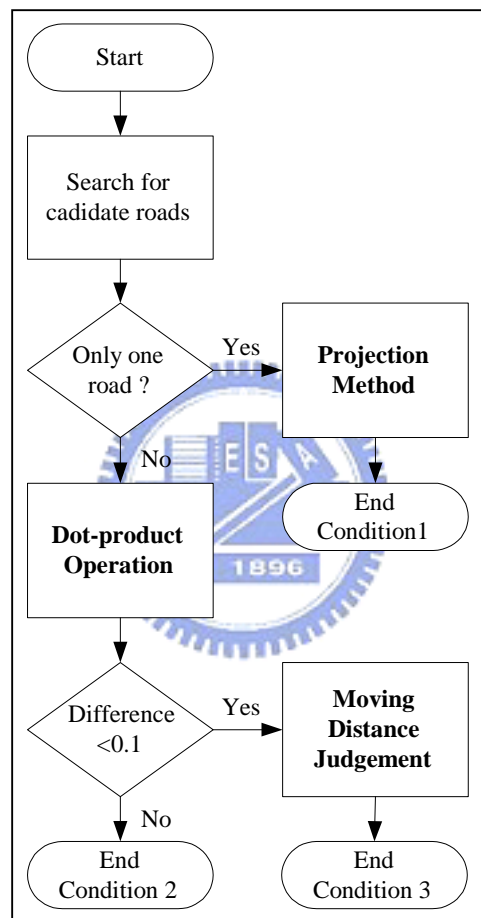


Figure 4.9 Searching mode flowchart

There are three conditions in the searching mode shown as figure 4.9. In condition2, there are 7 steps to match the right road shown as figure 4.10:

1. Search the candidate roads in the range of 20 m.
2. List the candidate roads (road1 and road2).
3. Find out the projected points according to two roads ($c_1(k), c_2(k)$).
4. Transfer to the unit vector form.

$$\bar{p}(k) = \frac{p(k) - p(k-1)}{\|p(k) - p(k-1)\|} \quad (4.4.1)$$

$$\bar{c}_1(k) = \frac{c_1(k) - s(k-1)}{\|c_1(k) - s(k-1)\|} \quad (4.4.2)$$

$$\bar{c}_2(k) = \frac{c_2(k) - s(k-1)}{\|c_2(k) - s(k-1)\|} \quad (4.4.3)$$

5. Perform the dot-product operation and find out the biggest one.

$$\bar{p}(k) \bullet \bar{c}_1(k) > \bar{p}(k) \bullet \bar{c}_2(k) \quad (4.4.4)$$

6. The $c_1(k)$ and road1 are chosen to be the matched point and matched road.

From figure 4.10, there are two candidate points $c_1(k)$ and $c_2(k)$ and they are almost possible to be the matched point. As the dot-product is applied, it is clear that the $c_1(k)$ is the right matched point.

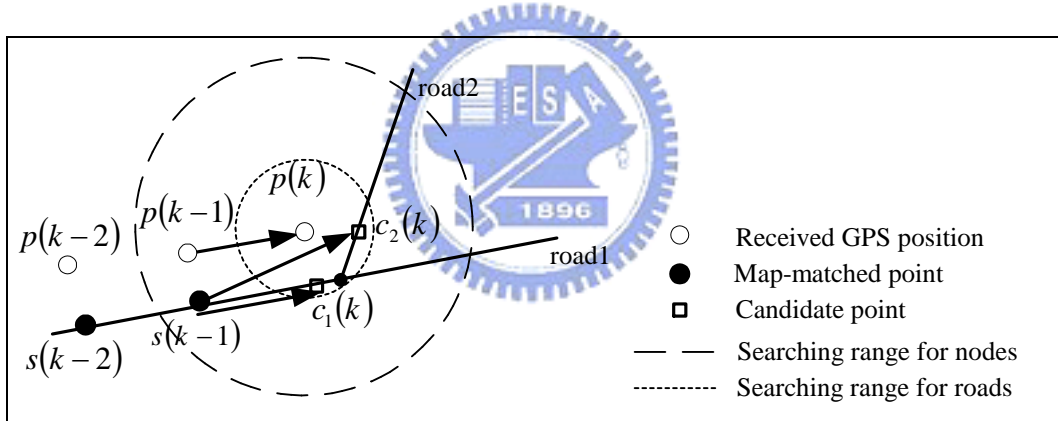


Figure 4.10 Condition 2

In condition 3, the moving distance judgment is adopted to decide the matched point and road finally. From the figure 4.11, the difference between $\bar{p}(k) \bullet \bar{c}_2(k)$ and $\bar{p}(k) \bullet \bar{c}_1(k)$ is smaller than 0.1, but when the moving distance judgment is used as:

$$\|c_2(k) - s(k-1)\| - \|p(k) - p(k-1)\| > \|c_1(k) - s(k-1)\| - \|p(k) - p(k-1)\| \quad (4.4.5)$$

Consequently, the $c_1(k)$ and road1 are decided as the matched point and road. The overall searching mode has been presented; the next section would introduce the tracking mode employed as there is no node near the vehicle.

4.4.5 Tracking Mode

As map-matching function enters the tracking mode, this expresses that there is only one road. Therefore, the matched road would be the initial road from the initial mode or the previous road. Furthermore, the projection method is applied to decide the matched point on the tracking road shown as figure 4.11. The entire map-matching algorithm has been expressed in section 4.4, and the performance of this algorithm would be tested in the experiment described in section 5.5.

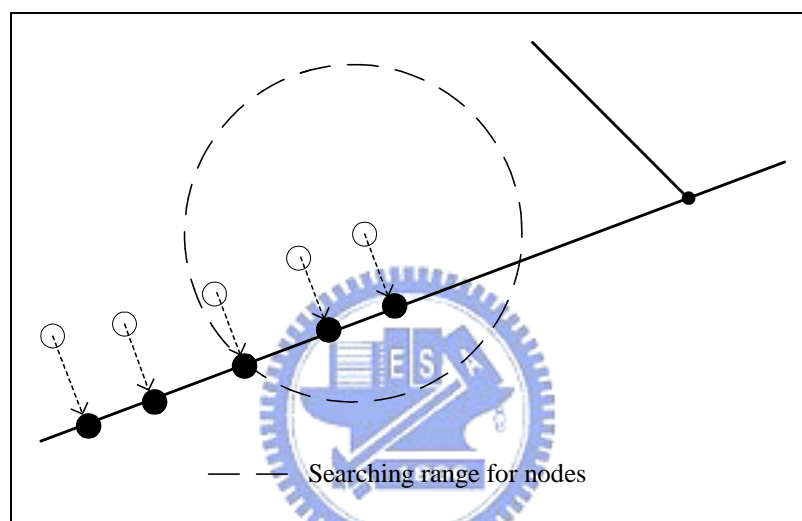


Figure 4.11 Tracking mode

Chapter 5 Integration of GPS/INS/GIS

5.1 Motivation

With the description of previous sections, it is clear that GPS, INS and GIS have complementary characteristics. These characteristics, which motivate the integration of navigation system, can be summarized as [22]:

- I. Accuracy: Due to the integral of acceleration and angular rate involved, as estimating position, the INS would produce unbounded grown error over time. This gives the requirement in correcting the errors periodically by external sensor. GPS, with bounded measurement errors, can be used to accomplish this work. Furthermore, GIS has most accurate precision database, which can associate GPS to improve the accuracy.
- II. Data Output Rate: The data output rate of GPS is generally 1Hz that can't satisfy the request of autonomous control of vehicle. The INS output rate can be higher, but the only limit being the ability of data processor. Therefore, the integration of GPS and INS is sufficient for the data output rate requirement.
- III. Data Availability: GPS is a radio-navigation system, and consequently its measurement is subject to the signal outage, interference, and jamming. On the contrary, INS is a self-contained and much immune to surrounding environment. Hence, INS can provide available and continuous navigation information when GPS loss signal in short-term time. On the other hand, GIS may disable while roadways have been developed or pulled down, and furthermore the GIS database has not update recently. However, GPS/INS would show the trajectory that vehicle passed through but the roadway

doesn't exist in GIS database.

As the compensated characteristics of each element have been presented clearly, the integration of GPS/INS/GIS would be possible to achieve a more efficient, robust, and accurate position estimate.

5.2 Integration Mode

In this application, there are three components of navigation, GPS, INS, and GIS, whose characteristics are complementary. In order to achieve the optimal performance, such as availability, reliability, and accuracy, the proposed procedure is to integrate them. The overall integration would be divided into two parts, one is GPS/INS and the other one is GPS/INS/GIS. As absolute position has been determined in GPS/INS, then the relative position in map would be matched from GPS/INS/GIS.

In GPS/INS integration, one Kalman Filter, which would be introduced in section 5.3, is used to combine two different data output rate systems, GPS and INS. Figure 5.1 shows the integration procedure that as the INS estimates the $P+\delta P$ and GPS measures the $P'+\mu$, and then the difference would be input into the Kalman Filter to get the optimal error dP' . After that, the output of INS may subtract the optimal error and get the optimal navigation.

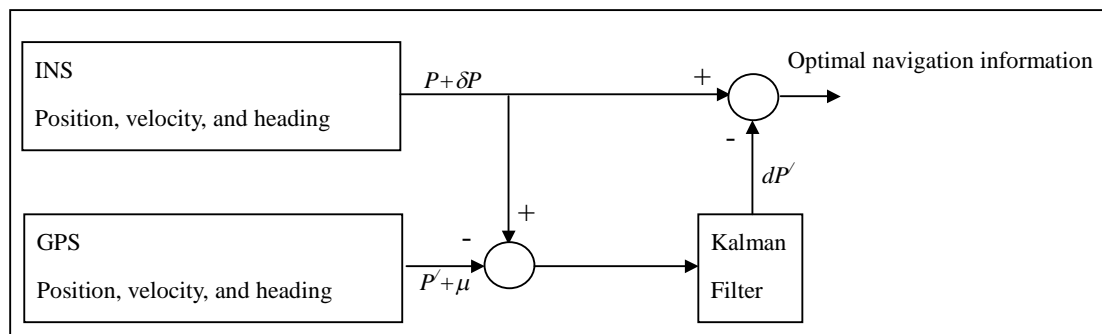


Figure 5.1 GPS/INS integration scheme

While the position, velocity, and heading direction shown in figure 5.1 have

been estimated, the next work would make effort in providing the correct geographic information for driver. Compare GPS, INS, and GIS, the GIS database is the most accurate due to the precise data establishment, thus the GIS is considered to fix the GPS/INS position. While using the map-matching algorithm, a GIS position correction method is proposed to fix the position determined from GPS/INS. If the absolute positions of GPS/INS just match to the relative positions on the road without correcting from GIS, the GPS/INS estimation error would cause the wrong matching shown as figure 5.2.

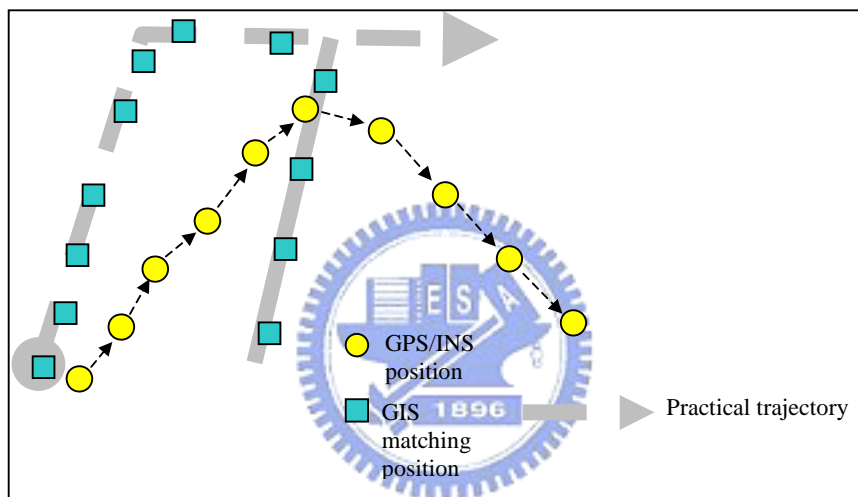


Figure 5.2 GPS/INS without GIS fix

Thus, the proposed method would match the present GPS/INS position to the correct position on the located road, and then the next heading direction estimation would be determined base on the heading direction measured from GIS shown in figure 5.3 (b). Since the vehicle runs in the road, the heading direction is similar to the direction of the road. The direction of road would be used to fix the heading direction. However, as the vehicle has a turn, the GIS heading direction fixing would fail and be shown as the left of figure 5.4. Because the direction of road doesn't vary as the vehicle run in the same road. Therefore, an improved method is to detect if there is a node near the vehicle and the variation of direction measured from INS; if yes, then the GIS heading direction fixing wouldn't work until there isn't node near the vehicle

and the vehicle and the variation of direction from INS is small. This method is shown in the figure 5.4 (b).

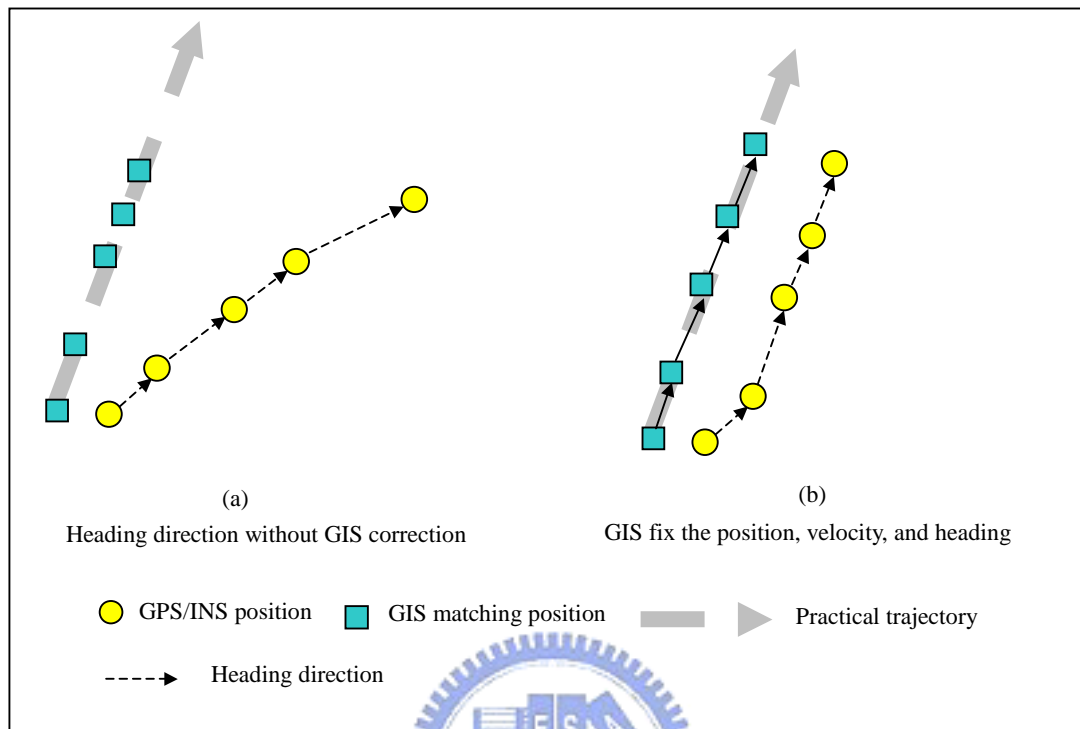


Figure 5.3 GIS fix GPS/INS

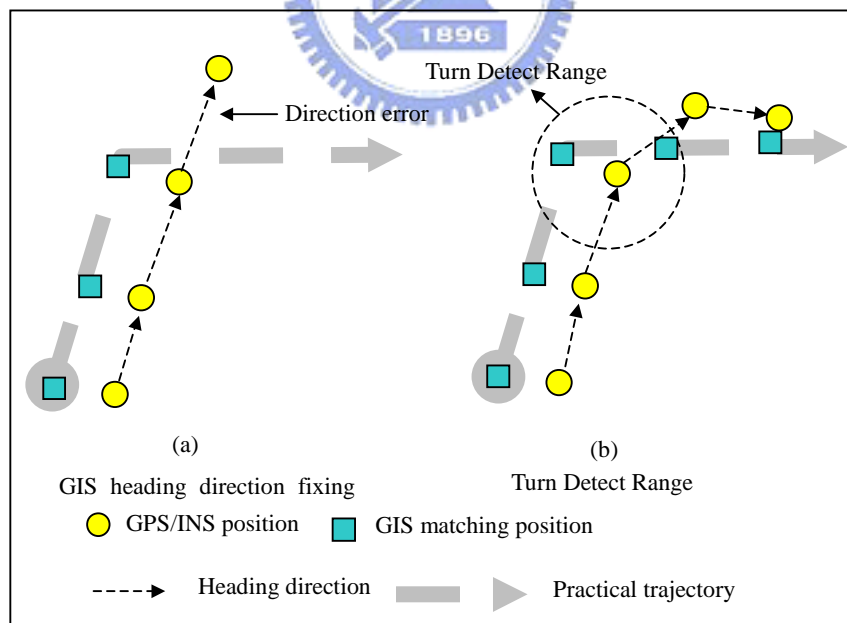


Figure 5.4 Turn Detect Range

As the heading direction has been fixed with GIS, the trajectory would be shown as figure 5.5. This trajectory of GPS/INS/GIS shows the more correct road information than the one of GPS/INS. Furthermore, as the GIS aid the GPS/INS, there

would be two conditions in real environment shown as in figure 5.3. As GIS is available, i.e. the road that the vehicle passes through exists, there would not be any error message.

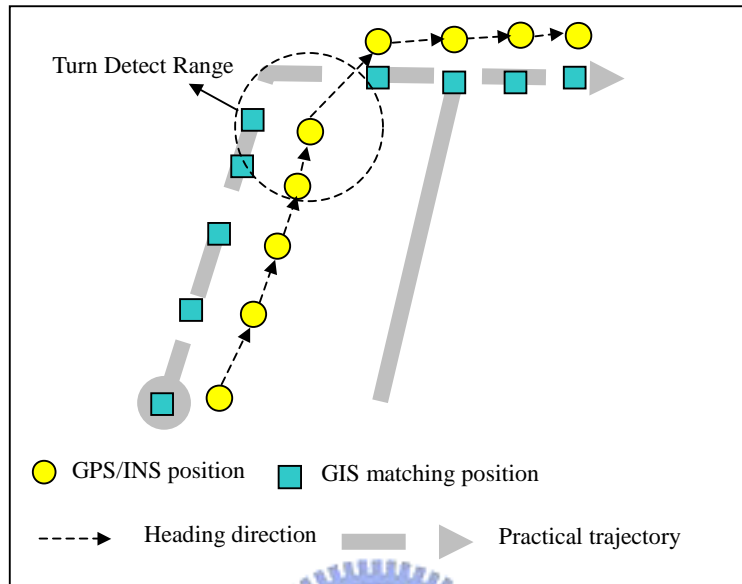


Figure 5.5 GIS fix GPS/INS

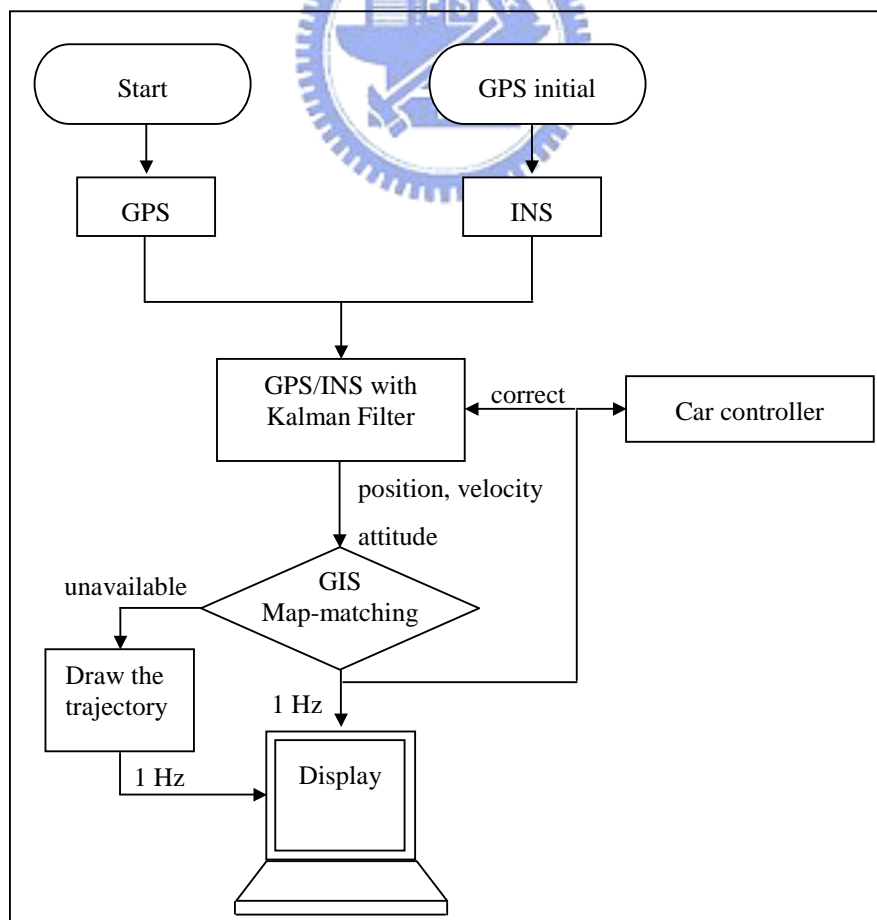


Figure 5.6 GPS/INS/GIS integration mode

However, if the vehicle passes through the road that have not been updated in GIS database, the navigation information would depend on the GPS/INS and show the trajectory without the located road information. Figure 5.6 interprets the overall integration mode, and further the output of GPS/INS, such as position, velocity, heading direction, could be also used in car control.

5.3 Filter Design

In navigation system, it is required for estimation to obtain position, velocity and attitude, modeled in (3.3.19) and (3.3.20). Further using psi-angle approach results in error models as shown in (3.4.11). In order to achieve the best estimates, most researchers relied on Kalman Filters, which is a recursive algorithm and requires external measurements to compute optimal corrections of system state variables. This application also includes a GPS as the external measurement, possessing tens of meters in position uncertainty. Thus, the main work of GPS/INS would be devoted to the design of the Kalman Filter, which provides the optimal navigation information.

5.3.1 Discrete Linear Dynamics Model and Observation Model

Consider the INS reduced error model in (3.4.11) that is a nonlinear system, and is needed to reformulate discrete-time form for Discrete Kalman Filter. In error model, it is assumed that for small time intervals, the dynamic matrix A' is constant. The state-transition matrix Φ is given as: [3]

$$\Phi = e^{A'\Delta t}. \quad (5.3.1)$$

Identifying $t_0 = t_{k-1}$ and $t = t_k$, and then the discrete random process \mathbf{u}_k with Gaussian, zero-mean white noise is given by

$$\mathbf{u}_k = \int_{t_{k-1}}^{t_k} \Phi(t, t') \mathbf{B}'(t') dt'. \quad (5.3.2)$$

Thus, the discrete error model can be given by

$$\delta \mathbf{X}'_k = \Phi(t_k, t_{k-1}) \delta \mathbf{X}'_{k-1} + \mathbf{u}_k. \quad (5.3.3)$$

The \mathbf{X}'_k and \mathbf{u}_k posteriori density are Gaussian and their covariance are respectively given as

$$\mathbf{P}_k = E(\mathbf{X}'_k \mathbf{X}'_k{}^T), \quad (5.3.4)$$

$$\mathbf{Q}_k = E(\mathbf{u}_k \mathbf{u}_k{}^T). \quad (5.3.5)$$

In (5.3.3), it describes the discrete linear dynamics model in a small time interval and would estimate the error state by sensed values from integrating the IMU sensor output.

Except for estimating error state by error model, the external measurement, GPS, can also obtain more accurate error at 1Hz. In this application, $\delta \mathbf{Y}_k$ might be the difference between measurement in GPS and estimation in INS, and they are also 5 observations linearly related to the state through the matrix \mathbf{H}_k shown as following:

$$\delta \mathbf{Y}_k = \begin{bmatrix} r_N^{GPS} - r_N^{INS} \\ r_E^{GPS} - r_E^{INS} \\ V_N^{GPS} - V_N^{INS} \\ V_E^{GPS} - V_E^{INS} \\ \psi^{GPS} - \psi^{INS} \end{bmatrix} = \mathbf{H}_k \delta \mathbf{X}'_k + \mathbf{v}_k. \quad (5.3.6)$$

$$\mathbf{H}_k = \begin{bmatrix} 1 & 0 & 0 & 0 & 0 & 0 & \cdots & 0 \\ 0 & 1 & 0 & 0 & 0 & 0 & \cdots & 0 \\ 0 & 0 & 1 & 0 & 0 & 0 & \cdots & 0 \\ 0 & 0 & 0 & 1 & 0 & 0 & \cdots & 0 \\ 0 & 0 & 0 & 0 & 1 & 0 & \cdots & 0 \end{bmatrix}_{5 \times 10}.$$

$$\mathbf{v}_k \sim N(0, \mathbf{R}_k)$$

where V_N^{GPS} is the north velocity measured from GPS and V_N^{INS} is the north velocity estimated from INS. In order to estimate the optimal error estimation, Kalman Filter combines the observation model with dynamic error model to integrate them.

Consequently, the estimation of state error using the observations is called the update, and the step based on the system dynamics error model is called the prediction.

5.3.2 Optimal State Vector Estimation

Before starting to compute the optimal estimation, some important symbols would be given expositions. An estimate of the state error is denoted with “ $\hat{\cdot}$ ”. There would be a distinction between if an observation were included. Let $\delta \hat{\mathbf{X}}'_k$ be the estimate at time t_k , just after including the observation $\delta \mathbf{Y}_k$; and let $\delta \hat{\mathbf{X}}'^{-}_k$ be the estimate just prior to the inclusion of the observation. With these preliminaries, optimal estimation can be started in two steps: prediction and filtering.

In many applications, the true values of system states are not known. However, it is assumed that the mean of the initial optimal estimate is known and given as

$$\delta \hat{\mathbf{X}}'_0 = \mathbf{E}[\delta \mathbf{X}'_0] \quad (5.3.7)$$

With the same assumption, the initial covariance of the system is

$$\mathbf{P}_0 = \mathbf{E}[\delta \mathbf{X}'_0 \delta \mathbf{X}'_0{}^T] \quad (5.3.8)$$

For convenience in further discussion, the errors in estimation can be shown as

$$\mathbf{e}_0 = \delta \hat{\mathbf{X}}'_0 - \delta \mathbf{X}'_0 \quad (5.3.9)$$

where

$$\mathbf{e}_0 \sim N(0, \mathbf{P}_0).$$

The states and errors ($\delta \hat{\mathbf{X}}'_k, \mathbf{e}_0$) are assumed to be Gaussian.

According to the state transition matrix, Φ , the states can be propagated to the expected value based on all prior information.

$$\begin{aligned} \delta \hat{\mathbf{X}}'^{-}_k &= \mathbf{E}[\delta \mathbf{X}'_k] \\ &= \Phi(t_k, t_{k-1}) \mathbf{E}[\delta \mathbf{X}'_{k-1}] + \mathbf{E}[\mathbf{u}_k] \\ &= \Phi(t_k, t_{k-1}) \delta \hat{\mathbf{X}}'_{k-1} \end{aligned} \quad (5.3.10)$$

where $\delta \hat{\mathbf{X}}_k'^-$ is the estimate error state in prediction prior to the use of new information and this is the known prediction. Then, let the estimation error be

$$\mathbf{e}_k^- = \delta \hat{\mathbf{X}}_k'^- - \delta \mathbf{X}_k' \quad (5.3.11)$$

Similarly, the estimation error and its covariance are propagated from (5.3.10), thus the error is

$$\mathbf{e}_k^- = \Phi(t_k, t_{k-1}) \mathbf{e}_{k-1} + \mathbf{u}_k \quad (5.3.12)$$

Covariance matrix of error would start to determine from \mathbf{P}_0 .

$$\begin{aligned} \mathbf{P}_k^- &= \mathbf{E}[\mathbf{e}_k^- \mathbf{e}_k^{-T}] \\ &= \Phi(t_k, t_{k-1}) \mathbf{E}[\mathbf{e}_{k-1}^- \mathbf{e}_{k-1}^{-T}] \Phi^T(t_k, t_{k-1}) + \mathbf{E}[\mathbf{u}_k \mathbf{u}_k^T] \\ &= \Phi(t_k, t_{k-1}) \mathbf{P}_{k-1} \Phi^T(t_k, t_{k-1}) + \mathbf{Q}_k \end{aligned} \quad (5.3.13)$$

Note that \mathbf{P}_{k-1} has non-negative diagonal elements, as dose \mathbf{Q}_k . Thus the variance of system states would increase due to the driving noise variance. Furthermore, the probability density of estimation error is Gaussian.

$$\mathbf{e}_k^- \sim N(0, \mathbf{P}_k^-) \quad (5.3.14)$$

A simple prediction is completed with available information, model, and gives the best estimation without external information.

Once new information is measured, it is important to employ this information to find the best estimate and then remove the error of prediction. This process is known as filtering. The best posterior estimate of error states based on the observation is combined with both the prior best estimate established in prediction and a weighting difference between the observation and the prior best estimate. In this thesis, the following algorithms will be adopted:

$$\delta \hat{\mathbf{X}}_k' = \delta \hat{\mathbf{X}}_k'^- + \mathbf{K}_k (\delta \mathbf{Y}_k - \mathbf{H}_k \delta \hat{\mathbf{X}}_k'^-) \quad (5.3.15)$$

$$\mathbf{P}_k = (\mathbf{I} - \mathbf{K}_k \mathbf{H}_k) \mathbf{P}_k^- (\mathbf{I} - \mathbf{K}_k \mathbf{H}_k)^T + \mathbf{K}_k \mathbf{R}_k \mathbf{K}_k^T \quad (5.3.16)$$

where

$$\mathbf{K}_k = \mathbf{P}_k^- \mathbf{H}_k^T (\mathbf{H}_k \mathbf{P}_k^- \mathbf{H}_k^T + \mathbf{R}_k)^{-1} \quad (5.3.17)$$

and then combined with (5.3.10)-(5.3.13) to establish the Kalman Filter, including prediction and filtering. The probability distribution of physical state variable $\delta \mathbf{X}'_k$ is Gaussian denoted as $N(\delta \hat{\mathbf{X}}'_k, \mathbf{P}_k)$. The matrix \mathbf{K}_k is known as the Kalman gain, which is analogous to a ratio of observation to prior information. Furthermore, the difference of new information and expected value, $\delta \mathbf{Y}_k - \mathbf{H}_k \delta \hat{\mathbf{X}}'^{-}_k$, is treated as innovation that would affect the computation of Kalman gain. [2,3]

5.4 Navigation System Design

The navigation system consists of one GPS receiver interface, a two-dimension INS, and two-dimension GIS database. The brief descriptions of the instruments used in this application are given as following sections.

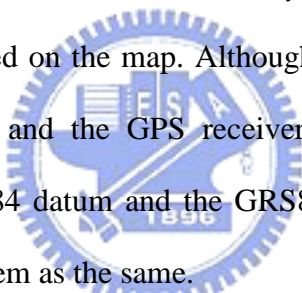
5.4.1 Hardware and Software

In hardware, a GPS engine board (GM-80-A) is employed to receive GPS signal that decoded and collected by using one microprocessor (8951) via RS232 protocol. The IMU set used in INS consists of one accelerometer (ADXL202) and one gyro (ENV-05A), and transform to digital with 12-bit A/D converter (MAX197). Then the other one microprocessor (8951) would receive the IMU digital signal directly and GPS data from the other microprocessor with 17 Hz, and then send them to main processor (Acer TravelMate 529ATX with Pentium 900 MHz).

In software, all the navigation functions constructed in main processor are developed in Visual Basic that is a useful developed environment and convenient to design real-time navigation system, and the GIS component, MapObjects [25], is also utilized in this environment. Furthermore, all the sensors data and GPS data are received with the Visual Basic interface.

The digital map structure includes seven kinds of map data, regions, railways, rivers, roads, bridges, landmarks and nodes. The developed component, MapObjects, uses the shapefile to show the map data on the graphic user interface. However, the raw data format of the map data is not the form shown as figure 5.7. Therefore, it is necessary to utilize the GIS software, MapInfo, to transfer the map file to the shapefile shown as figure 5.8.

In datum, the GPS receiver uses the WGS84 datum, and the longitude unit is *dddmm.mmmm* where *d* is degree and *m* is minute. However, the GRS80 datum and *x-y* coordinate are applied to the digital electronic map “TWD97TM2”. Therefore, the units are necessary to be transferred to degree. Then, using UTM projection to transfer longitude and latitude coordinates into the *x-y* coordinates. The data in the *x-y* coordinates would be displayed on the map. Although the digital map is constructed based on the GRS80 datum and the GPS receiver uses the WGS84 datum, the difference between the WGS84 datum and the GRS80 datum is very small, so that most researchers often treat them as the same.



	A	B	C	D	E	F	G	H	I
70	3051	RD042018	RD	0	1				大湖路
71	3057	RD042018	RD	0	1				大湖路
72	3158	AL051018	AL	0	1				大湖路147巷
73	3048	AL044018	AL	0	1				大湖路167巷
74	3062	AL044018	AL	0	1				大湖路167巷
75	3155	AL050018	AL	0	1				大湖路51巷
76	3156	AL050018	AL	0	1				大湖路51巷
77	717	RD090018	RD	0	1				大學路
78	722	RD090018	RD	0	1				大學路
79	723	RD090018	RD	0	1				大學路
80	841	RD090018	RD	0	1				大學路
81	842	RD090018	RD	0	1				大學路
82	848	RD090018	RD	0	1				大學路
83	721	AL106018	AL	0	1				大學路81巷

Figure 5.7 Raw Map Data Format

In order to replay the trajectory after the driver got home or the goal, an Access file is created to record the GPS/INS data and map-matching position, furthermore, the trajectory would be stored per second. Next section would describe the

programming procedure including initialization, navigation equation, and map-matching algorithm.

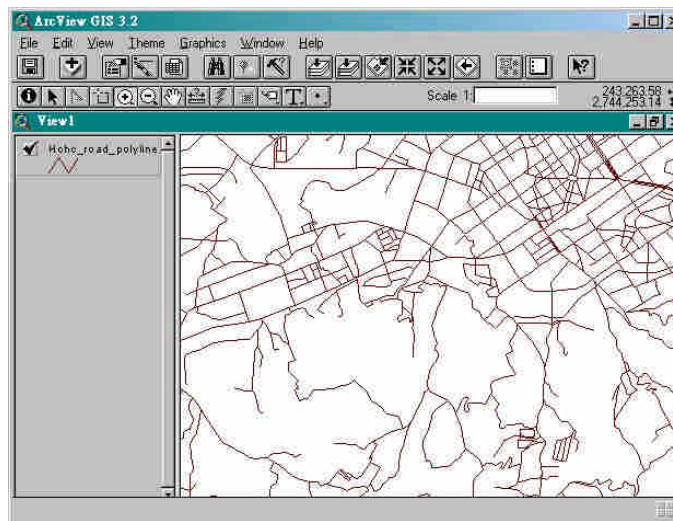


Figure 5.8 Shapefile in ArcView

5.4.2 Programming Procedure

After the hardware and software were represented, the next work would be devoted to design the navigation programming procedure. The procedure could be divided into two major parts, one is the data receive in two microprocessors; the other one is the data process in main processor. In two microprocessors, one is master and the other one is slave, the slave would handle the GPS message decode and data transmitting between the master and slave. The master would manage the IMU data, the sampling rate in the navigation system, and the interface between the master and the main processor.

The slave would receive the GPS message that is the word form, and then decode these words to the number of latitude and longitude per second. As the latitude and longitude have been decoded, the data would be transmitted to the master. Furthermore, the IMU outputs from sensors are analog signal, thus it is necessary to convert them to digital signal that could be processed in microprocessor. After using an A/D convert to completing this work, the master would handle the IMU digital

output, and then sends a request to the slave to get the GPS data. If GPS data were available, then the master would send GPS data and IMU data to the main processor with RS232 in 57600bps. However, if the GPS data were not available, the master would send the last GPS data. Figure 5.9 shows the data flowchart and how the master and slave work.

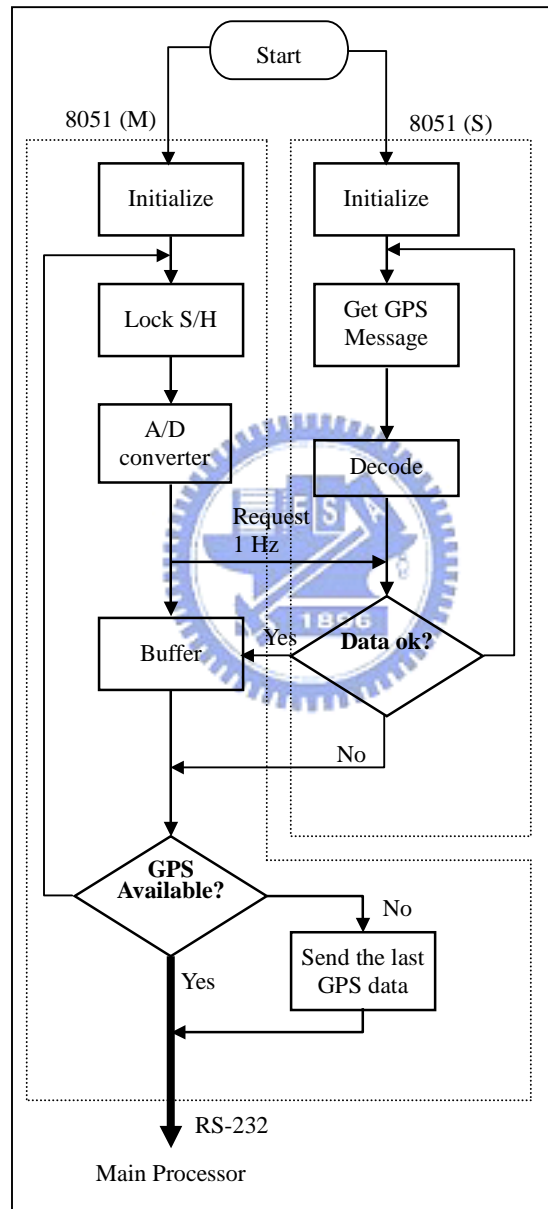


Figure 5.9 The data flowchart in two microprocessors

As the raw data has been transmitted to the main processor with RS232, the program developed with Visual Basic would start to process these data. The most important work of data process is to set the initial condition of the IMU data, since the

initial error would affect the further estimation and system performance far. The initial condition consists of position, velocity, and heading direction, which need to be estimated accurately.

The GPS positioning deviation is almost equal to 5 m and would not sometimes stable. Therefore, the initial heading direction measured from two nearby points would not be reliable and unstable, and isn't sometimes equal to the practical heading direction shown as figure 5.10 (a). As the INS integrated with GPS, the heading direction measured from GPS could not be used to correct the heading direction in INS. In order to solve this problem, a method that measures the heading direction from 1st and 5th points and obtains the continuous stable heading direction is proposed. Measuring heading direction from two nearby points may not suitable due to the unstable characteristic in short-term time. The proposed method shown as figure 5.10 (b) is to measure two points whose time interval is longer. As there are five GPS points, the 1st and 5th points are chosen to measure the heading direction ψ_1 , and ψ_2 is measured as the same method. While the ψ_1 , ψ_2 , ψ_3 , and ψ_4 are measured, they may not, however, practical due to the fact that one of them ψ_3 may be the error shown as figure 5.11 (c). Thus, in order to determine the practical heading direction, the proposed method obtains a stable heading direction from several continuous past heading directions shown as figure 5.11 (d). If these past angles were almost the same, then the last angle ψ_4 would be the initial heading direction. If they had large difference as figure 5.11 (c), the method would keep finding the stable heading direction as initial heading direction for INS.

After the heading direction initialization procedure, the initial position could be also obtained as the last position in heading direction initialization procedure. Since the position is considered as the stable position from GPS. Furthermore, as the initial position is given, the initial velocity would be accumulated from acceleration while

the system is started. The initial condition would be summarized as figure 5.11.

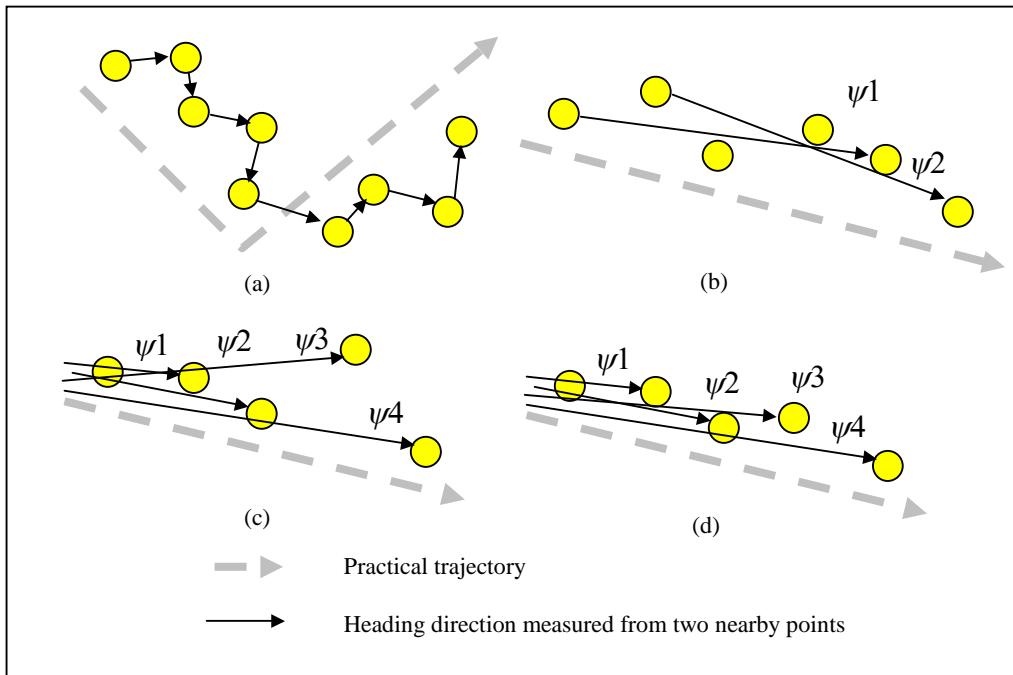


Figure 5.10 Heading direction estimation

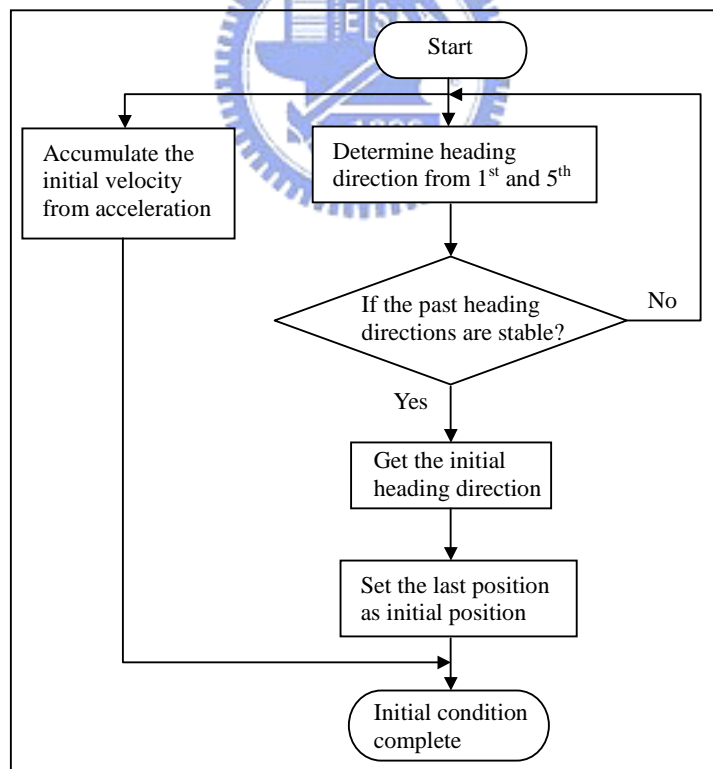


Figure 5.11 Initialize heading direction for INS

As the initial condition has been set, the next work would be devoted to estimate the position in the map. While the navigation works as the initial condition is given,

INS would be used to estimate the navigation information before the next GPS signal coming. As a new GPS signal is coming, the checking procedure would check that if this GPS signal were reliable. This checking procedure may employ the heading direction estimation to check the reliability of GPS data. If there were a strange GPS point P1 shown as figure 5.12 (a), i.e., the heading direction $\psi_{1'}$ is not similar to ψ_1 , the checking procedure would not treat P1 as reliable and keep determining the INS until GPS data gives a stable heading direction. Even though P1 locates near the turn and the vehicle would turn shown as figure 5.12 (b), the procedure would also treat P1 as unreliable and keep determining the INS. Since if the vehicle will turn, INS would detect and calculate the turn with less distortion. As a reliable GPS data is coming, the errors would be determined from subtracting the INS information from the GPS information. Then put these errors into the Kalman filter to calculate the optimal errors that would be subtracting from INS information shown as in figure 5.1. All the procedures described above just employ the GPS/INS, and further the GIS would be adopted to achieve the optimal navigation information.

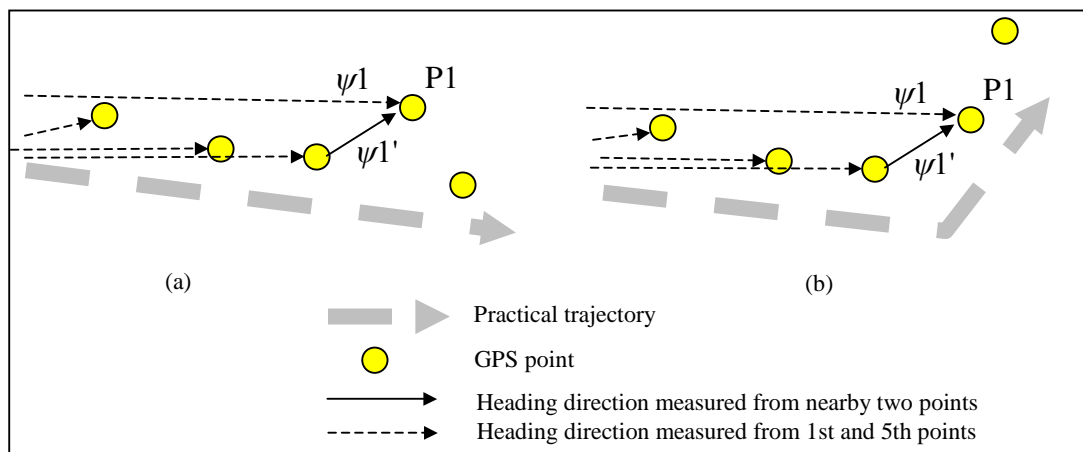


Figure 5.12 Check position reliability

The GPS/INS/GIS integration has been introduced in 5.2, and the GIS would be adopted as the method in 5.2. Except for direction correcting purpose, the GIS also could detect if the vehicle pass through the new road that doesn't exist in GIS

database. In the map-matching algorithm, the searching mode would detect if there were a road near the vehicle. If not, the origin procedure would locate the vehicle in the previous road. However, if the vehicle keeps going on this new road, the matching point would locate the almost same point due to the fact that matching road is the same. In order to improve this phenomenon, as the procedure enters the searching mode, if there were no road in GIS database, GPS/INS position would replace matching position and show on the map. Consequently, the driver would know the location of vehicle continuously and reliably.

5.5 Experiments

In order to test the performance of this navigation system, there are two experiment paths. Path 1 shown as figure 5.13 would pass through the underground passage, urban area, and wooded area, and these areas would test the GPS/INS/GIS performance while GPS signal is available and examine the INS/GIS performance when GPS signal is unavailable. Path 2 shown as figure 5.14 would be planned in National Chiao Tung University whose some roads doesn't exist and update in GIS database. Therefore, this path is useful to test GPS/INS performance without GIS correction.

Figure 5.15 shows the result of GPS/INS without the GIS correction, but the map-matching with GIS. The dash-line circle A and E in figure 5.15 shows the strange phenomenon of GPS that the longitude is static but the latitude varies, so that the trajectory would keep straight and vertical to parallel. However, the trajectory isn't towards the real path and would cause the error matching shown in dash-line circle A. Therefore, the most convenient and simple solution is to judge if the longitude is static, then the GPS signal would be classified to be unavailable.

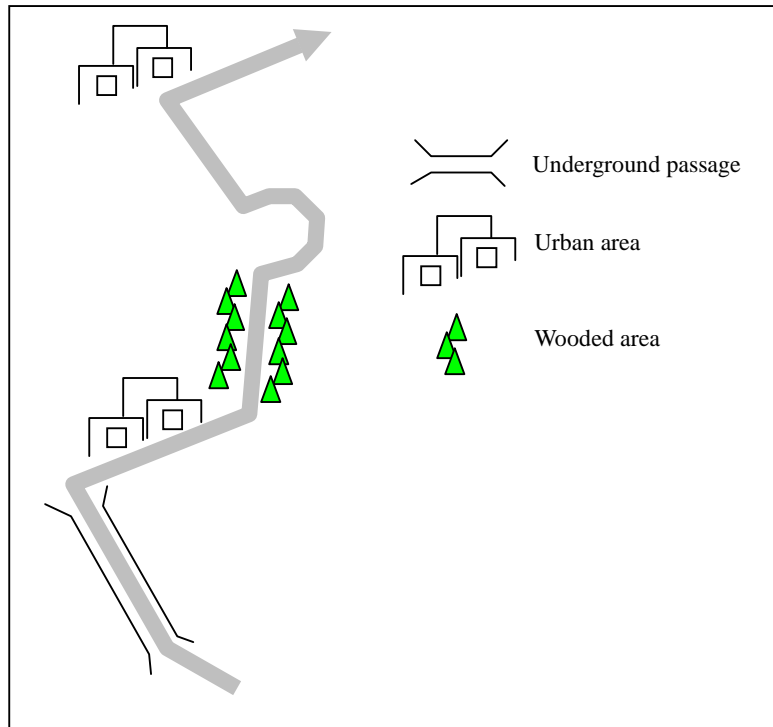


Figure 5.13 Path 1



Figure 5.14 Path 2

Since this phenomenon occurred at short-term time, it is reliable to depend on the INS/GIS in section A and E. In the section B, the vehicle pass through an underground passage, and then the vehicle turn right and enter an urban area. From the figure 5.15, there is no available GPS signal for GPS/INS and the heading direction strayed from the real path, so that the location was matched to the error road until the GPS

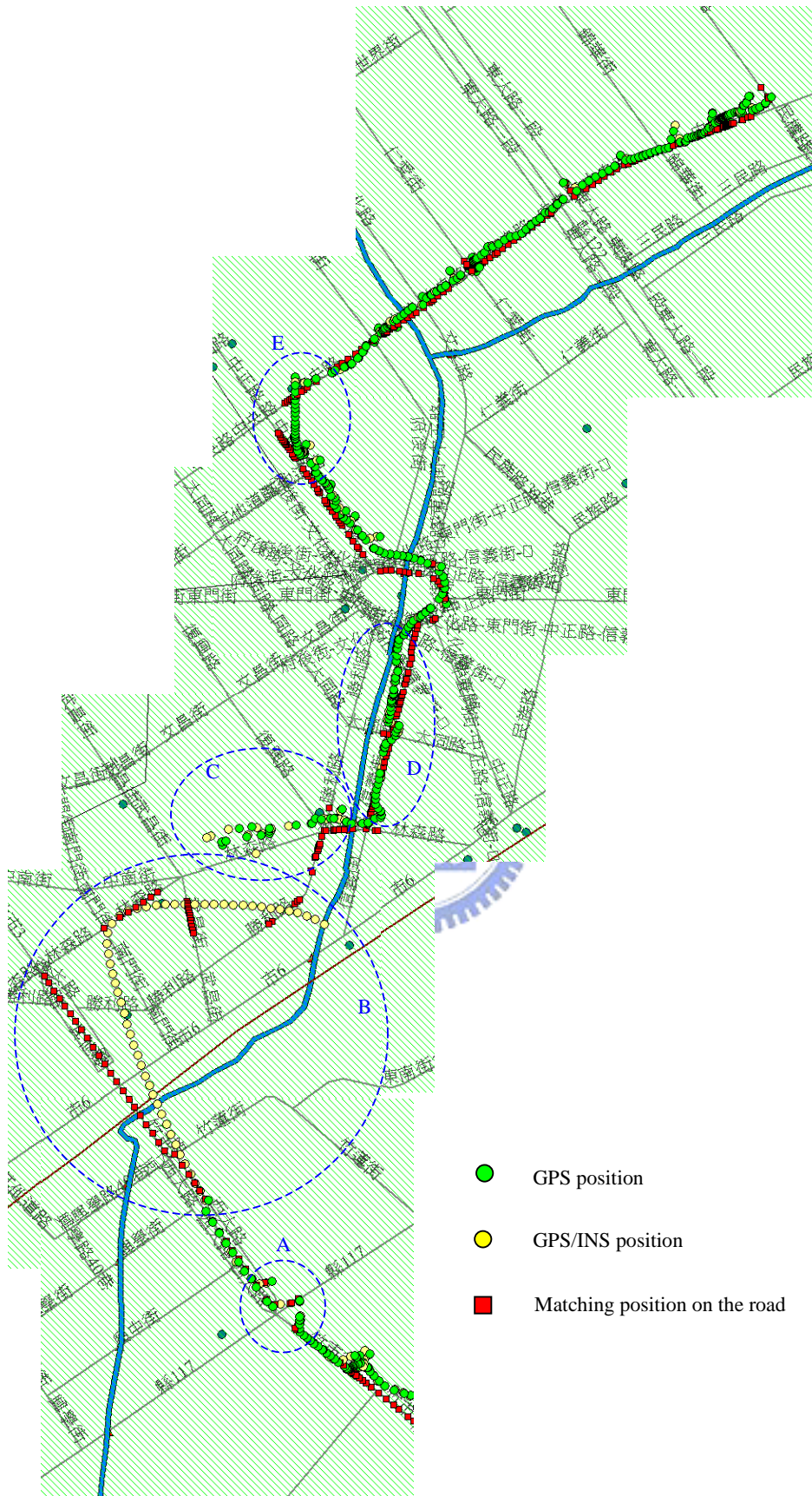


Figure 5.15 Path 1 result without GIS correction

signal was available in section C. However, the signals seemed to be untidy and the trajectory was rough, since there were more high buildings around the vehicle. In order to solve the phenomenon, the heading direction estimation shown in figure 5.10 and 5.12 would be adopted to smooth the trajectory for driver. There is a wooded area in Section D; the GPS signal, however, seemed to be available and was sometimes untidy in the middle of section D, so that the error matching would happen. This problem would be solved with the same method, heading direction estimation.

The path1 was experimenting with the modified procedure and the result is shown as figure 5.16. In the section A and E, the problem of strange GPS signal has been solved, so that the trajectory was smoother and there was no error matching. As the vehicle pass through the underground passage, the GIS aided the INS to correction the heading direction until the vehicle turned right. While the INS and GIS detected the node and turn, the INS would work without the heading direction aid from GIS. Therefore, the trajectory was smoother and more correct, and furthermore the matching was more correct.

While the GPS/INS/GIS performance and INS/GIS has been tested, the path 2 would be tested the performance of GPS/INS. Some roads in National Chiao Tung University are not updated in GIS database. Therefore, as the vehicle ran in the road shown as figure 5.17, the GIS would match the position to the other road where vehicle didn't run. While the matching positions were almost on the same location and the vehicle was moving, the GPS/INS position would be substituted for matching position shown as section B. Section C is a wooded area, so that the GPS signal was unavailable and INS should work alone. Even the INS worked without the aid of GPS or GIS, the trajectory was reliable and smooth due to the integration of acceleration and angular rate. The equipment employed in this experiment is shown as figure 5.18, the IMU set consists of one accelerometer and one gyro.

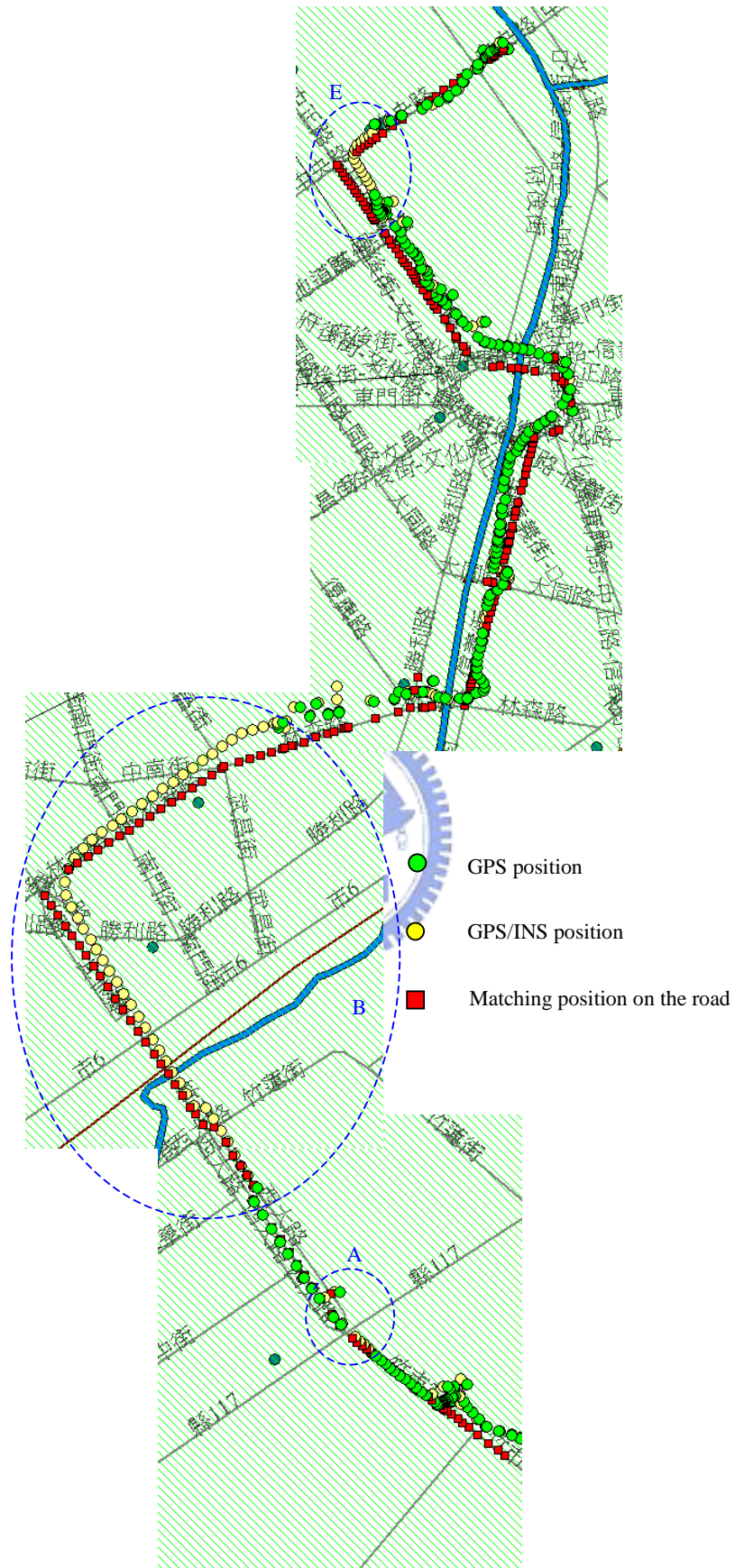


Figure 5.16 Path 1 result with GIS correction

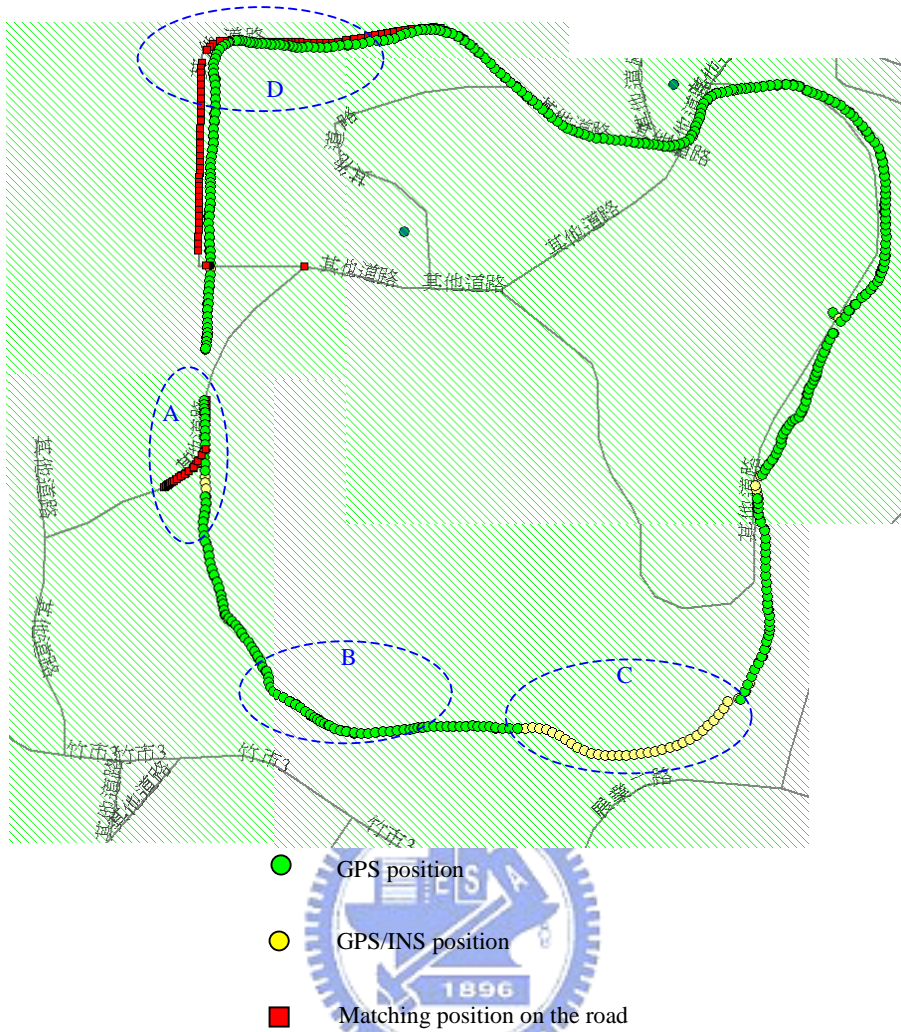


Figure 5.17 Path 2 result

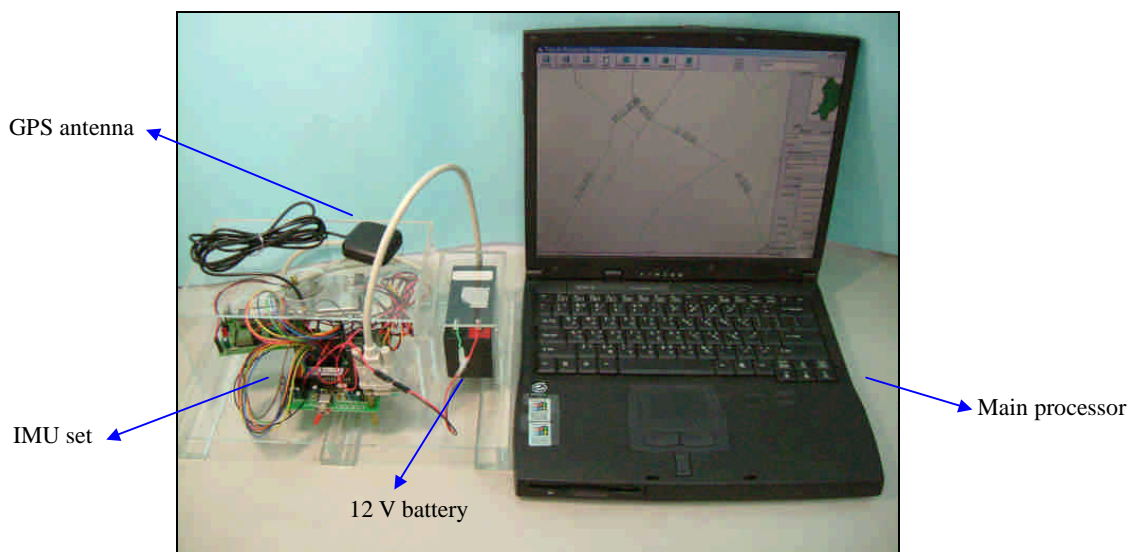


Figure 5.18 Experiment equipment

Chapter 6 Conclusions

This thesis mainly contributes to adopting Kalman filter to integrate GPS with INS and map-matching algorithm to integrate GPS/INS with GIS. In chapter 2, the pseudo range would be determined from the positioning equation. With the pseudo range and carrier phase, the absolute position of vehicle would be calculated. However, GPS is not always available for navigation. INS built up by a set of inertial measurement units (IMU) can provide continuous position and would not be affected by external interference. Therefore, in order to get continuous and smooth navigation information, INS introduced in chapter 3 is integrated with GPS. The coordinates of GPS and INS are different; thus, the position, velocity, and attitude of them need to integrate. Therefore, the required coordinate transformation is presented in section 3.2. In order to determine the navigation information in INS, the dynamic equation introduced in section 3.3 would be adopted to calculate this information. As determining this information from dynamic equation, the error caused from integration would accumulate and affect the performance of INS. Thus, the INS error model is derived to estimate the error. Then the Kalman filter presented in section 5.3 would be employed to integrate GPS/INS and estimate the error based on INS error model and observation model from GPS.

Even the GPS/INS is more accurate and reliable than GPS or INS alone, the absolute position from GPS/INS can't provide sufficient information for driver. GIS presented in chapter 4 would provide more accurate database to match the path. In this thesis, the position would be matched on the map in Taiwan coordinate. A map-matching algorithm, which includes initial mode, node nearby detection, searching mode, and tracking mode, would be used to match the position of GPS/INS to the correct road and point on map. This algorithm would provide the relative

position and the GIS provides the geographic information for driver.

As the system starts to navigate, the hardware constructed based on two microprocessors would receive the data that consists of acceleration and angular rate from INS and signal from GPS. Then these data would be transmitted to the main processor via RS232 interface. In the main processor, these GPS and INS data would be integrated with the conventional Kalman filter that is commonly adopted in navigation system to get optimal solution. As the map-matching algorithm is employed, there are still some matching errors due to the wrong computational heading direction. Therefore, a proposed heading direction correction method would compare and fit the trajectory of GPS/INS to the vehicle's real path. This proposed method would fail as the vehicle makes a turn. Therefore, a method that detects the node from GIS database and measures the variation of direction from angular velocity of vehicle is proposed to adjust the heading direction correction. Furthermore, as the vehicle runs in the road that doesn't exist and isn't updated in GIS database, a proposed strategy would detect whether there is a road near the vehicle or not. If yes, the GPS/INS position would replace the matching position. With the strategy, the navigation system would provide the reliable geographic information for driver. Consequently, with the experiments in section 5.5, the navigation system is flexible in different environments, even the underground passage, wooded area, urban area, and new built road. Furthermore, the results show these methods are feasible, and the trajectory is continuous, smooth, and reliable.

A flexible GPS/INS/GIS real-time navigation system has been proposed in this thesis. However, there are some drawbacks in this navigation system. One is that the road of GIS database is constructed based on the centerline of road, and the road in the map doesn't have the width. Therefore, the error of GIS database would depend on the width of roads. The other one drawback is that even the experiment tested the

performance of system in several different environments. However, there may be some strange environments, such as long tunnels, and the system may be fail in these environments due to the fact that the error in INS would accumulate, as GPS was unavailable for a long time. Another drawback is the small sampling rate due to the ability of main processor. As the navigation system would be adopted in autonomous vehicle control system, the sampling rate is too small to observe the dynamics.

Finally, the measurement error is poor to know and the GPS noise is not white Gaussian in practice. However, Kalman filter is implemented in the linear system and the noises of process and measurement are white Gaussian. Therefore, the estimated information from Kalman filter is not optimal. In order to solve this problem, some researchers adopt the adaptive Kalman filter to improve the poor knowledge of measurement error. [8] The adaptive Kalman filter would update the measurement error and the error estimation would be more accurate. However, the adaptive Kalman filter would take more computation time to estimate and update errors. In this thesis, the processor isn't able to fulfill the computation in time. Thus, in order to employ the adaptive Kalman filter, it is necessary to modify the entire algorithm used in this thesis. The future work will be devoted to modify the Kalman filter and map-matching algorithm to reduce the computation time and obtain more accurate navigation information.

Reference:

- [1] J. Farrell and M. Barth, *“The Global Positioning System and Inertial Navigation”*, McGraw-Hill, New York, 1998.
- [2] R. C. Brown and Y. C. Hwang, *“Introduction to Random Signals and Applied Kalman Filter”*, John Wiley & Sons, New York, 1997.
- [3] Christopher Jekeli, *“Inertial Navigation Systems With Geodetic Applications”*, Walter de Gruyter, Berlin, New York, 2001.
- [4] I. Y. Baritzhack and N. Berman, *“Control Theoretic Approach to Inertial Navigation System,”* Journal of Guidance, Control, and Dynamic, Vol.11, No.3, pp.237-245, 1988.
- [5] Nebot Eduardo, Sukkarieh Salah, and Durrant-whyte Hugh, *“Inertial navigation aided with GPS information”*, Mechatronics and Machine Vision in Practice, 1997 Fourth Annual Conference on Proceedings, pp.169 –174, 23-25 Sept. 1997.
- [6] Gordon, G.S, *“Navigation systems integration”*, Airborne Navigation Systems Workshop (Ref. No. 1998/275), IEE, pp.411 – 416,10 Feb 1998.
- [7] Liu Lichuan, Tian Zengshan, and Huang Shun-ji, *“An algorithm for integrating GPS/INS attitude determination system”*, Radar, 2001 CIE International Conference on Proceedings, pp. 167 –170, 15-18 Oct. 2001.
- [8] Christopher Hide, Terry Moore, and Martin Smith, *“Adaptive kalman filtering for low-cost INS/GPS”*, The Journal of Navigation, Vol. 56, pp.143-152, 2003.
- [9] 謝銘峰, *“GPS/DGPS 與慣性導航系統之整合研究”*, 國立交通大學控制工程研究所碩士論文, 1995.
- [10] 李忠隆, *“應用於車輛導航之 GPS/INS 整合系統設計”*, 國立交通大學電機與控制工程研究所碩士論文, 2000.
- [11] 紀佳宏, *“應用於即時車輛導航系統之 GPS/GIS 整合設計”*, 國立交通大學電機與控制工程研究所碩士論文, 2002.
- [12] 莊智清, 黃國興, *“電子導航”*, 全華科技圖書股份有限公司, 台北, 2001.
- [13] 黃國興, *“慣性導航系統原理與應用”*, 全華科技圖書股份有限公司, 台北, 1991.
- [14] 長天科技股份有限公司, *“HOLUX GM80/81 衛星接收模組使用手冊”*.
- [15] Analog Devices ADXL202 datasheet.
- [16] Murata ENV-05A datasheet.
- [17] A. Nautiyal, *“Algorithm to Generate Geodetic Coordinates from Earth-Centered*

Earth-Fixed Coordinates”, Journal of Guidance, Control, and Dynamic, Vol.11, No.3, pp.281-283, 1988.

- [18] Chi-Chang J. Ho, “*Overview of Navigation Theory*”, 26 Oct. 1994.
- [19] Jium-Ming Lin and Cheng-Wen Huang, “*Vehicle Navigation System Design by Integrating INS with GPS*”, National Symposium on Automatic Control, pp.453-458, 1998.
- [20] 林育平, 廖德誠, 蕭飛賓, 張瑞剛, “*飛行導航技術研究*”, 行政院國科會專題研究計畫成果報告, 1994, 1995.
- [21] 中正理工學院, “*全球定位系統與慣性導航研討會專輯*”, 15-16 May 1980.
- [22] J.Z. Sasiadek, Q. Wang, and M.B. Zeremba, “*Fuzzy Adaptive Kalman Filtering for INS/GPS Data Fusion*”, Proceedings of the 15th IEEE International Symposium on Intelligent Control (ISIC 2000), Rio Patras, Greece, pp.181-186, 17-19 July, 2000.
- [23] Keith A. Redmill, Takeshi Kitajima, and Umit Ozguner, “*DGPS/INS Integrated Positioning for Control of Automated Vehicle*”, 2001 IEEE Intelligent Transportation Systems Conference Proceedings, pp.172-178, Oakland (CA), USA, 25-29 Aug. 2001.
- [24] Michael Kennedy, “*The Global Positioning System and GIS: An Introduction*”, Ann Arbor Press, 1996.
- [25] ESRI.com, *MapObjects-Windows Edition*, <http://www.esri.com/>.
- [26] Environmental Systems Research Institute (Redlands, Calif.), “*Getting to know ArcView GIS: the geographic information system (GIS) for everyone*”, ESRI, 1999.
- [27] C. C. Chang and C. L. Tseng, “*A Geocentric Reference System in Taiwan*”.